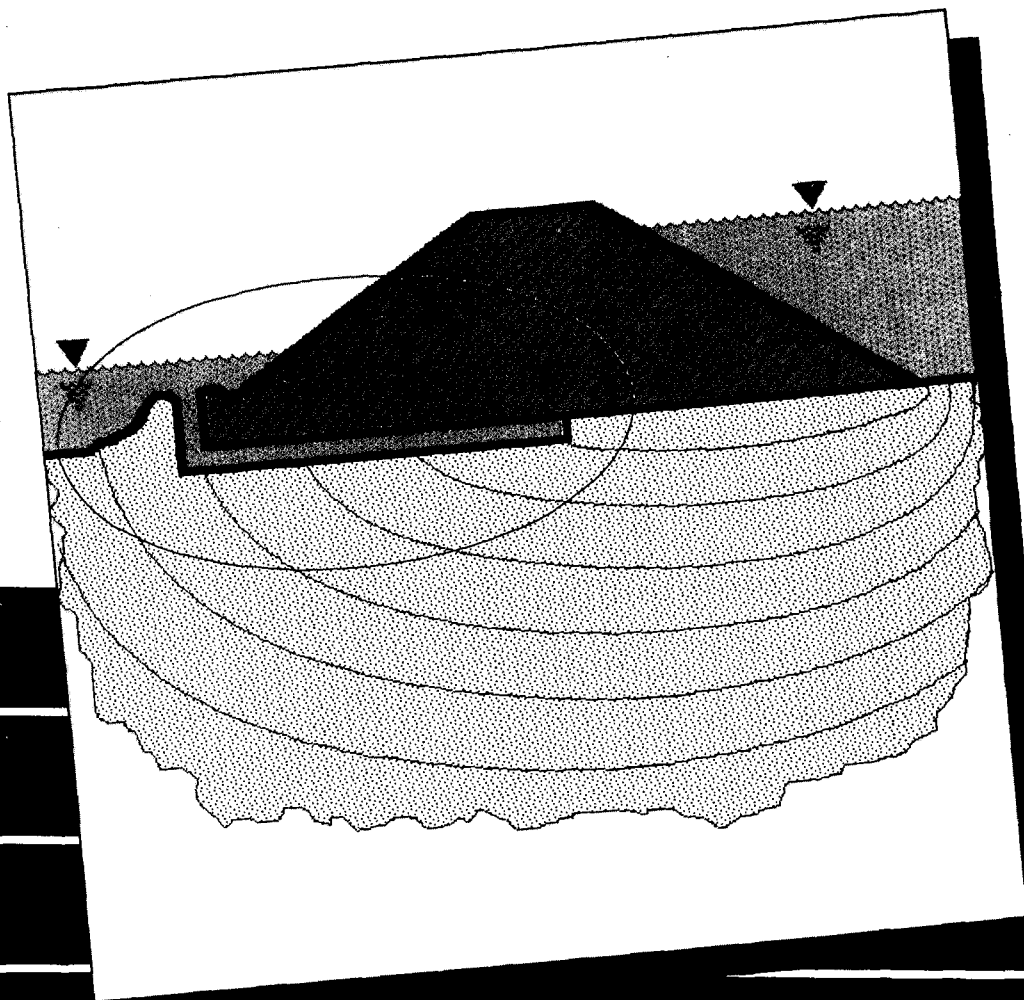


# ON THE MECHANISM OF PIPING UNDER IMPERVIOUS STRUCTURES



J.B. Sellmeyer

TR diss  
1670

# ON THE MECHANISM OF PIPING UNDER IMPERVIOUS STRUCTURES

461009  
517 88 80  
72 188 1670

J. B. SELLMEIJER

ON THE MECHANISM OF PIPING  
UNDER IMPERVIOUS STRUCTURES

Proefschrift



ter verkrijging van de graad van doctor  
aan de Technische Universiteit Delft,  
op gezag van de Rector Magnificus, Prof. Drs. P.A. Schenck,  
in het openbaar te verdedigen ten overstaan van een commissie  
door het College van Dekanen daartoe aangewezen,

op dinsdag 18 oktober 1988 te 14.00 uur

door

Joannes B. Sellmeijer

geboren te Amsterdam

civiel-ingenieur

TR diss  
1670

Dit proefschrift is goedgekeurd door de promotor

Prof. Dr. Ir. A. Verruijt

Stellingen bij het proefschrift

'On the Mechanism of Piping under Impervious Structures':

1. Het succes van de Oosterschelde Stormvloedkering heeft aangetoond dat het verplaatsingsgedrag van monolitische constructies zeer betrouwbaar geschat kan worden met behulp van een combinatie van normaal- en schuifveren.
2. Voor de toepassing van Geotextielen als belastingspreider bestaat een ontwerpregel, waarin zowel aan evenwicht als aan vormverandering is voldaan. Dit is bereikt door simulatie met een verend ondersteund membraan.
3. Wetenschappelijk onderzoek is in wezen ambivalent. Het heeft de neiging alles wat nog niet zichtbaar gemaakt is van de hand te wijzen, terwijl het juist de bedoeling van onderzoek is om iets te ontdekken wat nog niet bekend is.
4. In de huidige tijd wordt denken voornamelijk gerelateerd aan de ratio en is iets als intuïtie verdacht. Een onderwerp dat langer dan een halve eeuw meer intuïtief dan deductief bestudeerd is is piping. Er zijn geen gevallen bekend die hierdoor geleid hebben tot een catastrofe.
5. Het grootste probleem van wetenschappelijk onderzoek is het creëren van een helder begrippenkader. De natuurkunde is hier ondanks de stormachtige ontwikkelingen redelijk in geslaagd. In de psychologie kan men beter opnieuw beginnen.
6. De medische wetenschap heeft haar grootste successen geboekt op onderwerpen die relatief weinig aan de orde komen in een dokters spreekkamer.

7. Het is buitengewoon verontrustend te constateren dat in het vakgebied der psychologie aan de menselijke psyche een aanmerkelijk kleinere standaardafwijking wordt toegekend dan gewoonlijk voor grond gehanteerd wordt.
8. De woorden intelligent en intellectueel worden vaak gehanteerd als synoniem. Zij hebben echter eerder een tegenovergestelde betekenis. Een intellectueel is iemand die voor een trivialiteit een moeilijk woord verzint en daarom bijdehand lijkt. Iemand die intelligent is verklaart met eenvoudige begrippen gecompliceerde problemen en lijkt daarom dom.
9. Het toppunt van intellectualisme is het feit dat vijflettergrepig zichzelf omschrijft en tweelettergrepig niet. Overigens heeft alleen vijf deze eigenschap.
10. Anno 1988 wordt nog steeds niet algemeen ingezien dat, als twee opponenten bidden voor de overwinning, zelfs God er slechts één kan laten winnen.

Contents

Notation and list of symbols	VII
1. Introduction	1
2. Historical notes	3
3. Simple visual tests	5
4. Physical principles of the model	7
5. Groundwater flow	11
6. Limit state equilibrium in the sandboil	21
7. Flow in the slit	27
8. Limit state equilibrium in the slit	37
9. Evaluation	49
10. Design formula	57
11. Practical aspects	65
12. Conclusions	85
References	87
APPENDICES	
A. Derivation of hypergeometric shape functions	91
B. Application of hypergeometric shape functions	97
C. Elaboration of design formula	105

Notation and list of symbols

$A_n$	: Fourier coefficient
$C$	: surface factor
$\hat{C}$	: drag factor
$E$	: erosion factor
$H$ [m]	: hydraulic head across structure
$I, I_1, I_2$	: intermediate integration values
$L$ [m]	: length of structure
$P$ [m]	: head in sandboil and slit
$Q$ [m]	: discharge through slit per unit permeability
$R_e$	: Reynolds number
$R_{1,2,3}$	: reactions per unit volume and per unit weight of water
$S_{1,2,3,4}$	: soil forces per unit volume and per unit weight of water
$U, V$	: complex functions to describe flow in slit
$a(x)$ [m]	: depth of slit as function of position
$b$ [m]	: length of sandboil
$c$	: fabric parameter
$\bar{c}$	: fabric factor
$d$ [m]	: particle diameter
$e$	: void ratio
$f$	: auxiliary function
$g$ [m/s <sup>2</sup> ]	: gravitational acceleration
$h(x)$ [m]	: height of sandboil as function of position
$k$ [m/s]	: hydraulic permeability coefficient
$l$ [m]	: erosion length
$p$	: horizontal gradient in sandboil and slit
$q$	: vertical gradient in sandboil and slit (reversed)
$r$ [m]	: geometric integration variable
$s$	: normal force per unit volume and per unit weight of water
$t$	: shear force per unit volume and per unit weight of water
$u, v$ [m/s]	: slit velocity
$x, y$ [m]	: horizontal and vertical coordinates
$z$ [m]	: geometric plane



$\theta$	[DEG]	: internal friction angle of sand
$\hat{\theta}$	[DEG]	: bedding angle of sand
$\lambda$		: characteristic flow angle
$\Phi$	[m]	: head along geotechnical structure
$\alpha$	[DEG]	: branch angle
$\bar{\alpha}$	[DEG]	: conjugate branch angle
$\beta$		: shape factor
$\gamma_p$	[N/m <sup>3</sup> ]	: submerged unit weight of particles
$\gamma_s$	[N/m <sup>3</sup> ]	: submerged unit weight of sand
$\gamma_w$	[N/m <sup>3</sup> ]	: unit weight of water
$\delta$	[DEG]	: interparticle friction angle
$\epsilon$		: parameter in hypergeometric shape functions
$\zeta$		: transformed geometric plane
$\eta$		: imaginary axis of transformed geometric plane
$\theta$	[DEG]	: slope of sandboil
$\kappa$	[m <sup>2</sup> ]	: intrinsic permeability coefficient
$\lambda$		: flow angle
$\mu$		: auxiliary variable
$\nu$	[m <sup>2</sup> /s]	: kinematic viscosity
$\xi$		: real axis of transformed geometric plane
$\rho$		: normalized integration variable $r/\ell$
$\tau$	[N/m <sup>3</sup> ]	: drag force along slit bottom
$\hat{\tau}$	[N/m <sup>3</sup> ]	: shear stress in slit
$\phi$	[m]	: head
$\hat{\phi}$	[m]	: piezometric head in slit
$x$		: normalized horizontal ordinate $x/\ell$
$\psi$	[m]	: stream function
$\hat{\psi}$	[m]	: vorticity in slit
$\omega$	[m]	: complex potential
$\hat{\omega}$	[m]	: complex field
Re		: real part of complex number
Im		: imaginary part of complex number

indexing

0	: related to transition zone $x = 0$
b	: related to transition zone $x = b$
$\ell$	: related to transition zone $x = \ell$
m	: counter
n	: counter
$\epsilon$	: indicating hypergeometric contribution
—	: conjugate
^	: corresponding value in slit
~	: indicating weight of shape functions
~	: indicating normalization
`	: effective value
'	: differentiation with respect to actual variable

## 1. Introduction

In delta areas - as for example in large parts of The Netherlands - the land is protected from floods and high tides by dikes. In general these are constructed of impervious clays and built on a sandy aquifer as subsoil. Such structures are vulnerable to an erosion effect called piping. In this thesis a mathematical model is proposed which deals with the mechanism of piping. The model is basically analytical but employs a numerical method to refine the results. The outcome is presented in a standardised form to be used as a design rule.

Piping is a form of seepage erosion - the general name for the adverse effects of groundwater flow on soil stability. High seepage pressures may remove soil material to such an extent that geotechnical structures may, and do, collapse. Several terms have been used in the literature to classify this seepage erosion. For instance 'heave' ( a substantial soil volume which is simultaneously raised by seepage flow, Terzaghi (1967), V. Zyl (1981) ), 'karst-piping' ( the removal of material due to weathering, Dykhovichnyi (1979) ), 'hydraulic fracturing' ( the process of soil being locally pushed apart by porewater pressures, Seed (1981) ), and 'internal erosion' ( the transport of small particles through a matrix of larger ones, Lubochkov (1962), V. Zyl (1981) ).

The actual word 'piping' refers to the development of channels, which begins at the downstream side of the structure where the flow lines converge. Associated with this, high seepage pressure occurs. The subsequent erosion process develops backwards and due to the natural non-homogeneity in the soil the channels are irregularly shaped. If the process continues the structure may in the end collapse.

It is clear why this phenomenon should be studied: society's well-being and the economy are of nationwide interest. The safety of water retaining structures is these days being argued, especially

since design rules to date are empirical and appropriate to quite different geographical locations. Often they are inadequate.

The whole mechanism is quite complex and use is made of branches of soil mechanics (both continuum approaches and particulate aspects), groundwater flow and hydraulics. A certain amount of simplification has to be introduced so as to make the problem suitable for mathematical analysis. Inspiration is drawn from simple visual tests.

The model is essentially two-dimensional. It is believed that this does not seriously affect the validity of the results. The design rules obtained allow for a great variety of geotechnical conditions. The analysis gives insight into the safety factor of the design.

This thesis basically consists of three parts. The first one is formed by chapters 1 ... 4 and is meant as introduction and preparation for the modelling of the piping phenomenon. The second part is the modelling itself and is worked out in chapters 5 ... 10 and appendices A ... C. This portion is entirely of theoretical nature. The last part consists of chapter 11 which is mainly practical. It is meant as stand alone for engineers who do not care too much about theoretical elaboration, but are more interested in effective and economical design of water retaining structures.

## 2. Historical notes

Piping has been studied since the turn of the century. It is mentioned in the context of weir and dam design on sandy foundations where, in addition to the usual design problems encountered in civil engineering, seepage erosion plays an important role. As a result of research an empirical rule relates the hydraulic head across the structure,  $H$ , to the length of seepage,  $L$ . For simple structures  $L$  can be assumed to be equal to the length of the weir or dam. The rule reads as follows:

$$L = E H \quad (2.01)$$

where  $E$  is a coefficient that depends on the geometry and soil parameters.

The relation (2.01) appears in the work by Clibborn and Beresford (1902). Bligh (1910) followed this concept and defined  $L$  as seepage length, i.e. the length of the path along the structure that is followed by the groundwater. This same idea, also called line of creep method, was suggested by Griffith (1913). Another approach that has been advocated to some extent is called shortest path method, implying that  $L$  must be the shortest route the water can take under the structure.

So far investigations have referred only to small structures. Once the scale was enlarged, the value of  $L$  quickly exceeded realistic dimensions when referred to the length of the structure. Attempts were made to reduce this value artificially. Heel and toe sheetings were applied, and at the same time methods were refined to determine the groundwater flow pattern. Harza (1935) proposed the electric analogy method. Lane (1935) introduced the weighted seepage method in order to include the difference in horizontal and vertical permeability.

From a design point of view the use of heel and toe sheetings may be acceptable and there is no general objection to the use of the

type (2.01) rule. But it must be realized that in the case of a heel sheeting the character of the seepage erosion changes. The problem is no longer piping, but heave. In the literature there is often no clear distinction made between these two phenomena. Terzaghi (1967) for example talks about piping due to heave.

Up to the late 1970's research had been concentrated on the heel sheeting type of structure but piping had been mentioned in only a few articles. Laboratory tests were carried out in Germany and in The Netherlands. Miesel (1978) , Müller-Kirchenbauer (1978) and Hannes et al. (1985) performed model tests on piping from holes made at the top of a confined layer. De Wit et al. (1981) reported experiments in partly covered sand layers.

Theoretical methods which have contributed to the understanding of piping have been reported. Both Müller-Kirchenbauer (1978) and Sellmeijer (1981) used solutions for steady flow and applied conformal mapping; Hannes et al. (1985) worked with a numerical method. Seepage erosion is not an integral part of these calculations and so the actual mechanism is not adequately described. Nevertheless, it might be possible to use these solutions when designing against piping.

In this analysis a theoretical description is presented which does take the erosion mechanism into account.

### 3. Simple visual tests

As mentioned in the introduction the configuration under investigation is an impervious structure on top of a granular material. If the function of the structure is to retain water, groundwater flow will occur through the granular material due to the hydraulic head across the structure. It is known that piping takes place due to the effects of high seepage pressure on the downstream side of the structure. The question is how to describe this erosion problem.

In order to obtain qualitative understanding of the phenomenon simple laboratory visual tests have been carried out. A perspex container was filled with sand and partly covered by a perspex lid which simulates the impervious structure. The set-up is sketched in figure 3.1 where the applied hydraulic head is also indicated. During the tests the hydraulic head is gradually

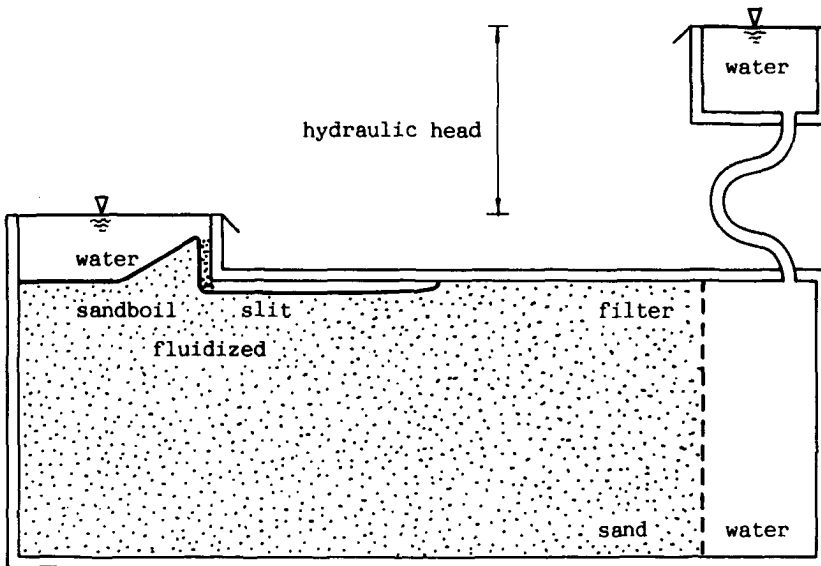


Fig. 3.1 : Model for laboratory test

increased in steps and the behaviour of the sand is observed.

At a certain stage it is noticed that sandboils appear in the outflow region. These "boils" consist of sand transferred from below the lid. The sand is fluidized in the center of the boils, allowing water to flow out. There is no net outflow of sand. But, if the hydraulic head is increased in a subsequent step, sand is transferred until again an equilibrium state is reached. Below the lid slits with a depth of several times the grain size develop. They look like meandering rivers which join up in an estuary.

It is obvious that the sandboils and slits limit the seepage pressures to a physically maximum possible level. Their height, length and depth increase with the hydraulic head. At a certain stage the seepage flow reaches a critical value which is associated with progressive erosion. At this point the seepage gradients apparently increase out of all proportion, unrestrained by changes in the flow pattern. The process then results in failure of the sandy aquifer.

These observations are the basis for a theoretical description of piping.



#### 4. Physical principles of the model

During the visual tests it was observed that in the presence of high seepage gradients sand is transferred from underneath the structure being tested to the outflow region. This process results in the appearance of sandboils and slits. It was noticed that equilibrium state conditions are possible as long as the sandboils and slits restrict the seepage gradients below a critical value. This critical value is believed to coincide with the point of failure of the sand. Beyond, progressive erosion begins and leads to the collapse of the geotechnical structure.

It is clear that the precise distribution of granular material in the outflow region is of great relevance to the analysis of piping. In figure 4.1 a plausible geometry - inspired by observations made in the tests - is shown. The sandboil is indicated by AB ; the slit by BC . At point B the sand is

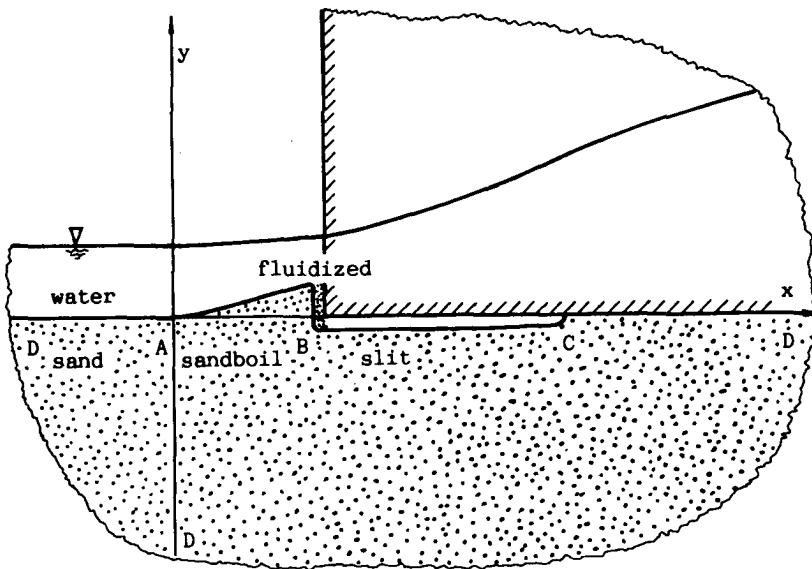


Fig. 4.1 : Plausible geometry in the outflow region

fluidized. The character  $D$  denotes infinity which mathematically speaking is an expanded point. The direction of the seepage flow is towards the free water surface.

In reality the problem is three-dimensional, however, to achieve the primary goal - a description of the mechanism of piping - a two-dimensional approach is presented. Such a description is believed to still capture the main mechanical features and not to invalidate the quality of the results. By implication it will now be impossible to include the meandering of the slits in the investigation. Meandering is due to the search for weak links in the granular structure of the sand. It is associated with the non-homogeneity of the sand properties and is therefore not an essential but an added feature of the piping problem.

During the visual tests it appeared that a new steady state seepage flow could be reached after an increase of the hydraulic head. This means that the steady state flow equation can be applied to describe the flow. Computational results, however, depend very much on the appearance of the sandboils and slits. Their geometry is erratic but can be simplified as follows.

The function of the slit is to conduct seepage water. Its depth is a few times the grain size and geometrically irrelevant. The sandboil provides resistance in the outflow region and therefore its dimensions do matter. But it is no problem to consider the seepage through AB in figure 4.1. Therefore the groundwater flow may be studied in the lower half-plane DABCDD. However, in addition the seepage in the sandboil itself must be determined.

The flow can be solved if the boundary conditions are known. At DA the head is constant due to the presence of the free water surface; at CD there is no vertical discharge, because the structure there is impervious. But at ABC the boundary conditions depend on the erosion process. During the visual tests it was observed that an increase in the hydraulic head caused some sand transport, resulting in a new steady state. Therefore, it is

plausible that this state is defined by the condition of limit equilibrium of the sand.

The problem now is how to incorporate this condition in the flow calculations. The following scheme proved fruitful: indicate the value of the head at ABC by the variable  $P$  ; then solve the groundwater flow expressing all important flow features in the yet unknown value  $P$  . Knowledge about the soil response can be used to evaluate the variable  $P$  .

It would appear that piping contains two features: seepage flow and limit equilibrium of the sand. The latter must be determined both in the sandboil and in the slit. In the following chapters these aspects will be elaborated upon and unified into one mathematical model to describe the phenomenon of piping.

## 5. Groundwater flow

One of the major mechanisms controlling piping appears to be groundwater flow. This may be studied in the lower halfplane DABCD of figure 4.1 . In this chapter the head of the groundwater flow will be determined under the following conditions: the flow is steady and is regarded as two-dimensional. The head is denoted by  $\phi$  being a function of the coordinates  $x$  and  $y$  . During calculations it turns out to be convenient to work with the gradient of  $\phi$  . Consequently the boundary conditions are expressed in this dimension. They are indicated in figure 5.1 which shows the same geometry as figure 4.1 .

At DA the value of the horizontal gradient  $\partial\phi/\partial x$  is zero due to the presence of the free water surface. At ABC the latter is indicated by  $p = dP/dx$  , where  $P$  represents the yet unknown value of the head. In a later stage this head will be defined by

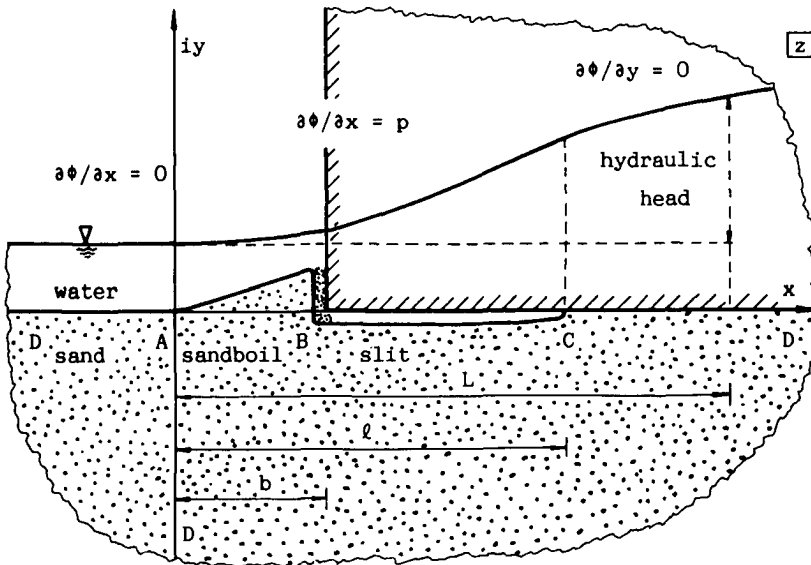


Fig. 5.1 : Geometry in the outflow region

the condition of limit equilibrium. At CD the vertical gradient vanishes, since no vertical discharge takes place.

The process of steady flow is characterized by the steady flow equation or Laplacean. For a homogeneous and isotropic coefficient of permeability this equation reads:

$$\left( \frac{\partial^2}{\partial x^2} + \frac{\partial^2}{\partial y^2} \right) \phi = 0 \quad (5.01)$$

The task is to solve equation (5.01) in the region of the lower halfplane DABCD for the afore mentioned boundary conditions, i.e.  $\partial\phi/\partial x = 0$  for  $x < 0$ ,  $\partial\phi/\partial x = p$  for  $0 < x < l$  and  $\partial\phi/\partial y = 0$  for  $x > l$ .

There are two suitable methods which lead to a solution. Both make use of the complex variable theory. To that end the geometrical plane in figure 5.1 will be described by the complex variable  $z = x + iy$ . Here  $i$  is the imaginary unit  $\sqrt{-1}$ . Also the head  $\phi$  will be extended with the stream function  $\psi$  to the complex potential  $\omega = \phi + i\psi$ . Usually in complex flow theory the head, stream function and complex potential are multiplied by the permeability coefficient and indicated by  $\Phi$ ,  $\Psi$  and  $\Omega$  respectively, but here these variables per unit permeability are preferred.

According to complex variable theory any analytical function  $\omega(z)$  contains a head  $\phi$  satisfying equation (5.01). That means that the problem is reduced to the determination of the boundary conditions only. Two methods to do so may be considered: the Cauchy integral formula and the theory of conformal mapping. These methods lead to perfectly equal answers in an entirely different mathematical representation.

At first the Cauchy integral formula will be dealt with. Polubarinova-Kochina (1962) presents an elaboration (chapter VI) of this formula appropriate to the present problem. The formula states that in case of a lower halfplane any analytical function  $f$  can be represented by:

$$f(z) = \frac{-1}{\pi i} \int_{-\infty}^{\infty} \operatorname{Re}[f(r)] \frac{dr}{r-z} \quad (5.02)$$

Re stands for real part,  $r$  is an integration variable along the line DABCD in figure 5.1 .

The equation (5.02) implies that boundary conditions in terms of  $f$  are available along the entire line DABCD . In order to meet the requirement for this problem a special function  $f$  is considered:  $d\omega/dz / \sqrt{(\ell-z)}$  , where  $\ell$  indicates the combined length of sandboil and slit, called erosion length. Thus the equation (5.02) is turned into,

$$\frac{d\omega/dz}{\sqrt{(\ell-z)}} = \frac{-1}{\pi i} \int_{-\infty}^{\infty} \operatorname{Re} \left( \frac{d\omega/dr}{\sqrt{(\ell-r)}} \right) \frac{dr}{r-z} \quad (5.03)$$

What is the advantage of the representation (5.03)?

In complex theory it is known that the derivative of  $\omega = \phi + i\psi$  is equal to  $d\omega/dz = \partial\phi/\partial x - i \partial\phi/\partial y$  . On the one hand, along the line DA where  $r < 0$  , the gradient  $\partial\phi/\partial x$  vanishes and thus the value of  $\operatorname{Re}[d\omega/dr / \sqrt{(\ell-r)}]$  is zero. On the other hand, along the line CD where  $r > \ell$  , the gradient  $\partial\phi/\partial y$  vanishes and therefore the value of  $\operatorname{Re}[d\omega/dr / \sqrt{(\ell-r)}]$  is zero too. Keeping in mind that for  $0 < r < \ell$   $\partial\phi/\partial x = p$  and  $\sqrt{(\ell-r)}$  is real, equation (5.03) may be rewritten as:

$$\frac{d\omega}{dz} = \frac{-1}{\pi i} \int_0^{\ell} p(r) \sqrt{\frac{\ell-z}{\ell-r}} \frac{dr}{r-z} = \frac{-1}{\pi i} \int_0^{\ell} p(r) \sqrt{\frac{\ell-r}{\ell-z}} \left( \frac{1}{\ell-r} + \frac{1}{r-z} \right) dr \quad (5.04)$$

For a proper function  $p$  this equation states that  $\omega$  is an analytical function of  $z$  and therefore  $\phi$  satisfies the flow

equation (5.01). Quite simply it can be checked that the boundary conditions have been met, and so equation (5.04) is a suitable representation of the solution of the flow equation (5.01). The expression for  $\omega$  itself follows by integration over  $z$ . To perform this integration the second integral of the right hand expression of (5.04) will be rewritten by partial integration with respect to  $r$ ,

$$\frac{d\omega}{dz} = \frac{-1}{\pi i} \int_0^{\ell} p(r) \sqrt{\frac{\ell-r}{\ell-z}} \frac{dr}{\ell-r} + \frac{+1}{\pi i} \int_0^{\ell} P(r) \frac{d}{dr} \left[ \sqrt{\frac{\ell-r}{\ell-z}} \frac{1}{r-z} \right] dr$$

Integration of the first integral over  $z$  is simple. The second integral shows a special property. Integration with respect to  $z$  compensates a great deal the differentiation with respect to  $r$ . This can be seen as follows,

$$\int \frac{d}{dr} \left[ \sqrt{\frac{\ell-r}{\ell-z}} \frac{1}{r-z} \right] dz = - \frac{1}{\ell-r} \int \frac{d}{d\left(\frac{\ell-r}{\ell-z}\right)} \left[ \sqrt{\frac{\ell-r}{\ell-z}} \frac{1}{1 - \frac{\ell-r}{\ell-z}} \right] d\left(\frac{\ell-r}{\ell-z}\right)$$

Therefore integration with respect to  $z$  results in,

$$\omega = \frac{2}{\pi i} \sqrt{(\ell-z)} \int_0^{\ell} p(r) \frac{dr}{\sqrt{(\ell-r)}} - \frac{1}{\pi i} \int_0^{\ell} P(r) \sqrt{\frac{\ell-z}{\ell-r}} \frac{dr}{r-z} \quad (5.05)$$

No integration constant is needed since the real part of (5.05) vanishes in  $z = 0$  and the imaginary part in  $z = \ell$ .

Formula (5.05) describes perfectly well the defined flow problem. It would appear that this equation is quite helpful for deriving certain particular shape functions to build up the total solution. However, general shape functions are better expressed differently. Another approach to the flow problem (5.01) will be tried from a different viewpoint.

A well-known method of solving complex potentials is transformation by conformal mapping. This method can be applied successfully. Now the geometrical  $z$ -plane is transformed into a strip. This strip, which is denoted by the complex variable  $\zeta = \xi + i\eta$ , is shown in figure 5.2. The letters A to D inclusive correspond with the ones in figure 5.1.

There is a one-to-one relationship between the original and the transformed plane. The form of an infinitesimal element remains unaltered; only the size and orientation change. Because of this, the term 'conformal mapping' is used. The relationship between the geometrical plane and the strip can be determined by the technique of Schwarz-Christoffel transformations, as described in, for example, Churchill (1960), Verruijt (1970). The result is as follows:

$$\zeta = 2/\pi \arcsin\sqrt{z/\ell} \quad (5.06)$$

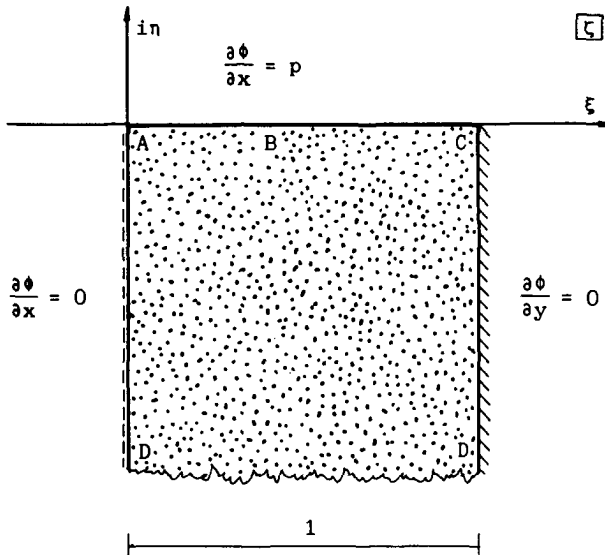


Fig. 5.2 : Transformed geometrical plane



In a strip the concept of Fourier series comes readily to mind and an exponential transformation of  $\zeta$  is obvious. Since CD is a streamline and DA an equipotential line the mapping function  $\exp\{\frac{1}{2}\pi i - (n+\frac{1}{2})\pi i\zeta\}$  is appropriate, for this function yields real values along CD and imaginary values along DA. In order to arrive at a solution which satisfies the condition along ABC, the Fourier series (5.07) is introduced:

$$\frac{d\omega}{dz} = \sum_{n=0}^{\infty} A_n \exp\{\frac{1}{2}\pi i - (n+\frac{1}{2})\pi i\zeta\} \quad (5.07)$$

In this representation the yet unknown horizontal gradient  $p$  is characterised by the coefficients  $A_n$ .

From equation (5.07) an expression for  $\omega$  can be determined by integration. In so doing, it is helpful to consider  $\omega$  as function of  $\zeta$  instead of  $z$ . From the transformation (5.06) it follows that,

$$\frac{dz}{d\zeta} = \frac{\pi}{2} \ell \sin(\pi\zeta) = -\frac{\pi i}{2} \frac{\ell}{2} \{\exp(\pi i\zeta) - \exp(-\pi i\zeta)\} \quad (5.08)$$

Thus, relation (5.07) may be written as:

$$\frac{d\omega}{d\zeta} = \sum_{n=0}^{\infty} A_n \frac{\pi}{2} \frac{\ell}{2} [\exp\{-(n-\frac{1}{2})\pi i\zeta\} - \exp\{-(n+\frac{1}{2})\pi i\zeta\}] \quad (5.09)$$

The function  $\omega$  is now easily obtained by the integration of (5.09) with respect to  $\zeta$ :

$$\omega = \sum_{n=0}^{\infty} A_n \frac{\ell}{4} \left[ \frac{\exp\{-(n-\frac{1}{2})\pi i\zeta\}}{-(n-\frac{1}{2})i} - \frac{\exp\{-(n+\frac{1}{2})\pi i\zeta\}}{-(n+\frac{1}{2})i} \right] \quad (5.10)$$

The expansion (5.10) also describes the flow problem very well. Basically the previous result (5.05) is different in that the function  $P$  there is the fundamental unknown to settle the flow problem, but here the solution is embedded in Fourier coefficients

$A_n$ . Fourier series are best used if the coefficients can be obtained from integration. If this is not the case, special care must be taken, particularly when the behaviour is not smooth. Solution (5.10) will be used as a set of general shape functions. Together with particular shape functions of a wilder nature through solution (5.05) they will construct the total solution.

Two results are now obtained, which describe the seepage problem perfectly well: the integral representation (5.05) and the Fourier series (5.10). They are identical, although mathematically they have an entirely different form. It is possible to prove by substitution that they are equal, but it is beyond the scope of this presentation to work this out.

From the results all relevant flow features may be obtained. In the sandboil and slit the following ones are considered: the horizontal and vertical gradients indicated by  $p$  and  $-q$  respectively; the head  $P$  and the discharge through the slit per unit of permeability denoted by  $Q$ ; and the head along the geotechnical structure indicated by  $\phi$ . The value of  $Q$  equals the reverse value of  $\psi$  for  $z = x$ , which represents the total discharge through the slit.

Since  $d\omega/dz = \partial\phi/\partial x - i \partial\phi/\partial y$ , the values of  $p$  and  $q$  simply equal the real and imaginary parts of equation (5.04) or (5.07) in the sandboil and slit. The following relations are obtained:

$$p = \frac{dP}{dx} = \sum_{n=0}^{\infty} A_n \sin\left[\left(n+\frac{1}{2}\right) \pi \xi\right] \quad (5.11)$$

$$q = \frac{1}{\pi} \int_0^{\ell} p(r) \sqrt{\left(\frac{\ell-x}{\ell-r}\right)} \frac{dr}{r-x} = \sum_{n=0}^{\infty} A_n \cos\left[\left(n+\frac{1}{2}\right) \pi \xi\right]$$

Here the value of  $\xi$  is specified by transformation (5.06),

$$\xi = 2/\pi \arcsin\sqrt{(x/\ell)} \quad 0 < x < \ell \quad (5.12)$$

If the pole  $r = x$  is involved, integration in (5.11) is carried out according to Cauchy's principle. The integral is also useful for  $x < 0$  without need of Cauchy's principle.

The values of  $P$  and  $-Q$  are equal to the real and imaginary parts of the potential  $\omega$  in the sandboil and slit. Therefore, with the aid of equations (5.05) and (5.10) the following holds:

$$P = \sum_{n=0}^{\infty} A_n \frac{\ell}{4} \left[ \frac{\sin\{(n-\frac{1}{2}) \pi \xi\}}{(n-\frac{1}{2})} - \frac{\sin\{(n+\frac{1}{2}) \pi \xi\}}{(n+\frac{1}{2})} \right] \quad (5.13)$$

$$\begin{aligned} Q &= - \sum_{n=0}^{\infty} A_n \frac{\ell}{4} \left[ \frac{\cos\{(n-\frac{1}{2}) \pi \xi\}}{(n-\frac{1}{2})} - \frac{\cos\{(n+\frac{1}{2}) \pi \xi\}}{(n+\frac{1}{2})} \right] \\ &= \frac{2}{\pi} \int_0^{\ell-x} p(r) \frac{dr}{\sqrt{(\ell-r)}} - \frac{1}{\pi} \int_0^{\ell} P(r) \sqrt{\frac{\ell-x}{\ell-r}} \frac{dr}{r-x} \end{aligned}$$

The obtained results (5.11) and (5.13) may be checked by the conditions  $p = dP/dx$  and  $q = -dQ/dx$ .

The derived quantities  $P$ ,  $Q$ ,  $p$  and  $q$  concern the sandboil and slit. Besides, the head along the structure is of importance too, because at a distance  $L$  from the outflow region this head represents the hydraulic head. Its value is directly obtained from the real part of the relation (5.10), realizing that at CD in figure 5.1 the value of  $\zeta$  is in the range,

$$\zeta = 1 + i\eta = 1 - i \frac{2}{\pi} \operatorname{arccosh} \sqrt{x/\ell} \quad x > \ell \quad (5.14)$$

$$\text{with, } \exp(-\frac{1}{2}\pi\eta) = \sqrt{x/\ell} + \sqrt{x/\ell - 1}$$

The integral representation is simply equal to the real part of (5.05). For the head  $\phi$  along the structure then the following relation is arrived at,

$$\begin{aligned}\Phi &= \sum_{n=0}^{\infty} (-1)^n A_n \frac{\ell}{4} \left[ \frac{\exp\{(n+\frac{1}{2}) \pi n\}}{(n+\frac{1}{2})} - \frac{\exp\{(n-\frac{1}{2}) \pi n\}}{(n-\frac{1}{2})} \right] \\ &= \frac{2}{\pi} \int_0^{\ell} \sqrt{(x-\ell)} p(r) \frac{dr}{\sqrt{(\ell-r)}} - \frac{1}{\pi} \int_0^{\ell} P(r) \sqrt{\left(\frac{x-\ell}{\ell-r}\right)} \frac{dr}{r-x}\end{aligned}\quad (5.15)$$

The value of  $n$  is determined by relation (5.14).

The groundwater flow is sufficiently described by the equations (5.11), (5.13) and (5.15). Both representations, the integral equation and the Fourier expansion will be used in the numerical elaboration.

Complex calculus leads to a solution for the groundwater flow field in an elegant manner. To include the sandboil in the description - thereby slightly modifying the geometry - an analytical continuation is put forward. Here particularly the power of the complex variable method is apparent, since it may be simply written,

$$\frac{d\omega}{dz} = \frac{\partial \phi}{\partial x} - i \frac{\partial \phi}{\partial y} = p(z) + i q(z) \quad (5.16)$$

The boundary conditions are satisfied because for  $z = x$  it holds that  $\partial \phi / \partial x = p(x)$  and  $\partial \phi / \partial y = -q(x)$  and the steady flow equation is valid too, as long as  $p(z)$  and  $q(z)$  are analytic functions.

At the leading edge there are two flow features and one geometric property to be determined: the horizontal and vertical gradients and the height of the boil as function of position  $h(x)$ . On the surface of the sandboil the head  $\phi$  vanishes. This requirement will lead to a condition for  $h(x)$ . The equality  $\phi = 0$  is equivalent to  $\text{Re}\{\omega(x+ih)\} = 0$ . To obtain  $h$  in explicit form this equation may be differentiated with respect to  $x$ . Using the chain rule, the following is arrived at,

$$\operatorname{Re}\left\{\left(\frac{\partial \phi}{\partial x} - i \frac{\partial \phi}{\partial y}\right) \left(1 + i \frac{dh}{dx}\right)\right\} = 0$$

or,

$$\frac{dh}{dx} = - \left(\frac{\partial \phi / \partial x}{\partial \phi / \partial y}\right)_{(y=h)} \quad (5.17)$$

This is not a surprising result; it implies that the flow lines are perpendicular to the surface of the sandboil.

The right-hand side of equation (5.17) is determined by (5.16). Though compactly expressed this equation is actually quite complicated. However, it is sufficient to consider a first order approach to the problem and to assume,

$$\frac{\partial \phi}{\partial x} \approx p(x) \quad \frac{\partial \phi}{\partial y} \approx -q(x) \quad (5.18)$$

Automatically the above-mentioned flow features are found now. With the aid of equation (5.17) the following approximate value of  $h$  is obtained:

$$\frac{dh}{dx} \approx \frac{p(x)}{q(x)} \quad h \approx \frac{P(x)}{q(x)} \quad (5.19)$$

Relations (5.18) and (5.19) are sufficient to proceed to describe stability characteristics, as will be shown in the following chapter.

## 6. Limit state equilibrium in the sandboil

Sandboils are due to particle transport caused by outflowing groundwater. In the previous chapter this flow is well described assuming a yet unknown distribution of the head in the sandboil and slit. In this chapter a condition will be derived in order to fix this head in the sandboil. It will appear later that the characteristics of the sandboils do not influence the ultimate result very much. Yet, if sandboils are not taken into account it is not possible to describe the piping process as a stable one. This will be demonstrated at the end of this chapter. At the juncture of sandboil and slit a gradient is required to move water from the slit. The presence of the sandboil takes care of this.

Information on the stress state in the sandboil is necessary so as to determine the groundwater flow. The sand is believed to be in a state of limit equilibrium. A general calculation of the stresses in the sandboil is quite intractable but a simplified approach will lead to manageable and realistic results. In figure 6.1 an element KLMN at the surface of the sandboil is considered. It contains a great number of sand particles, so that the principles of continuum mechanics may be applied.

The following forces per unit volume and per unit weight of water act on this element:

- submerged unit weight of the soil element per unit weight of water,  $\gamma_s^*/\gamma_w$  ;
- horizontal gradient of the seepage flow; according to relation (5.18) a first order approximation is  $p$  ;
- vertical gradient of the seepage flow; according to relation (5.18) a first order approximation is  $-q$  ;
- normalized force at the bottom of the element, resolved into a vertical component,  $S_1$  , and a component parallel to LM ,  $S_2$  ;
- normalized force at the left side of the element,  $S_3$  ;
- normalized force at the right side of the element,  $S_4$  .

The normal force per unit volume and per unit weight of water is indicated by  $s$ , the shearing force per unit volume and per unit weight of water is denoted by  $t$ . The sand has an angle of internal friction,  $\theta$ . The slope angle,  $\theta$ , is related to the height  $h(x)$  by the equation  $\tan\theta = dh/dx$ . As a first order approach equation (5.19) yields the relation:

$$\tan\theta = \frac{dh}{dx} = \frac{p}{q} \quad (6.01)$$

The system of soil forces  $S_1 \dots S_4$  is statically undetermined and information from the entire field is required, which would demand finite element type calculations. But, if the influence of variations along the surface of the sandboil is neglected, the system can be forced into a unique solution. To this end the forces at the right and left sides of the element will be supposed to be of equal magnitude and opposite direction.

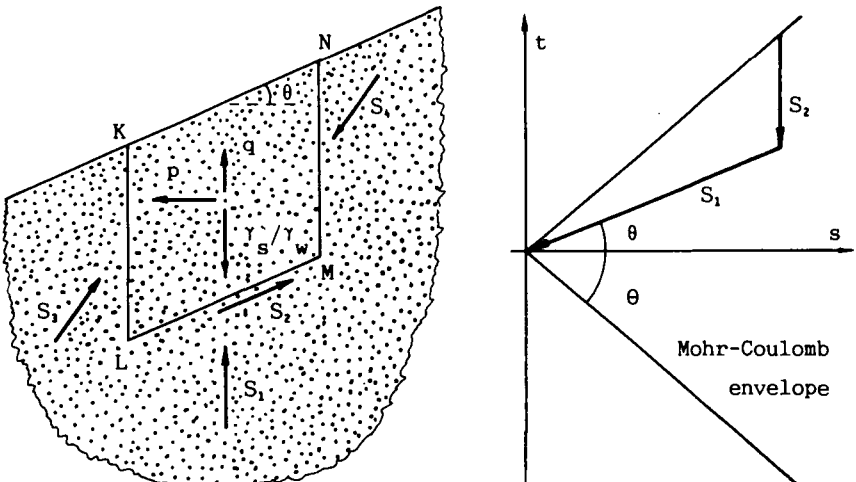


Fig. 6.1 : Stress state in the sandboil

The soil forces per unit volume and per unit weight of water at LM are now specified. Horizontal and vertical conditions of equilibrium of the soil element KLMN result in the following:

$$S_1 = \gamma_s' / \gamma_w - q - p \tan \theta \quad (6.02)$$

$$S_2 = p / \cos \theta$$

These forces are related to each other by the condition of limit equilibrium. If the soil is in a limit stress state then the effective soil force must lie on the Mohr-Coulomb envelope as plotted in the s-t diagram in figure 6.1 . Applying the sine law this gives the following relation between  $S_1$  and  $S_2$ :

$$\frac{S_1}{\sin(\frac{1}{2}\pi - \theta)} = \frac{S_1}{\cos \theta} = \frac{S_2}{\sin(\theta - \theta)} \quad (6.03)$$

Substitution of equations (6.02) into condition (6.03) relates the horizontal and vertical gradient to the slope angle,

$$\{\gamma_s' / \gamma_w - q - p \tan \theta\} \sin(\theta - \theta) = p \cos \theta / \cos \theta$$

or,

$$\gamma_s' / \gamma_w = q + p \cot(\theta - \theta) \quad (6.04)$$

This simple relation together with (6.01) describes the limit stress state of the sandboil. Elimination of the slope angle by substitution of (6.01) yields a relation between  $p$  and  $q$  only:

$$\frac{q + p^2 / q}{1 - p / q \cot \theta} = \frac{\gamma_s'}{\gamma_w}$$

Since this equation is based on a first order approximation the quadratic term is not appropriate. Without it, the final result is as follows:



$$\gamma_w/\gamma_s q + p/q \cot\theta = 1 \quad (6.05)$$

It is indeed a simple formula. However, it should be noted that this relation is not linear. Condition (6.05) will be used to determine the values of the head in the sandboil.

It is interesting to visualize the relation (6.05) between  $p$  and  $q$ . For this purpose this equation is rearranged as,

$$\gamma_w/\gamma_s p \cot\theta = \frac{1}{2} - (\gamma_w/\gamma_s q - \frac{1}{2})^2 \quad (6.06)$$

The relation obviously represents a parabola, as shown in figure 6.2. The influence of the slope of the sandboil is given by the difference between the straight line and the parabola. It is seen that the maximum value of  $p$  is  $\frac{1}{2} \gamma_s/\gamma_w \tan\theta$ .

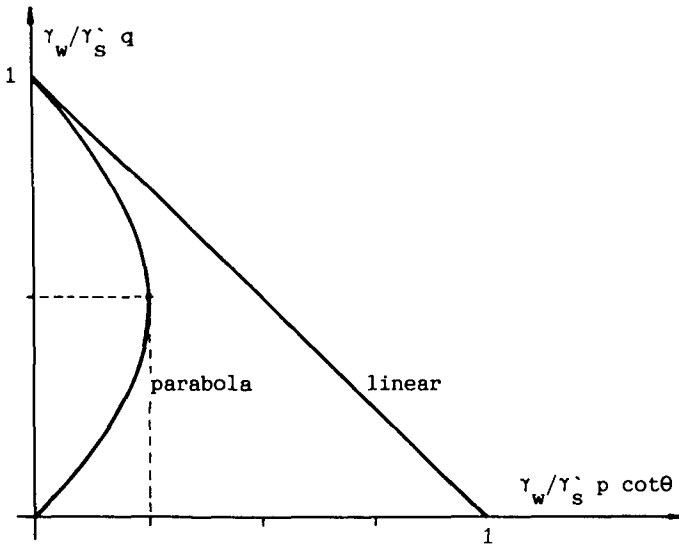


Fig. 6.2 : Relation between  $p$  and  $q$  in the sandboil

The necessity of the sandboil for the stability of the problem is now easily understood. Without it  $p$  is discontinuous, as its value vanishes along line DA while a gradient in point B is required for the water to flow out of the slit (see fig. 4.1). According to (5.11)  $q$  would become infinite then, thus violating (6.05). Now that it is present  $q$  remains finite and a solution for (6.05) is always possible for continuous  $p$ .



## 7. Flow in the slit

The sandboil in the outflow region is a result of material which has been moved from underneath the structure. This erosion process is associated with the formation of a slit. As the slit becomes longer, locally the permeability increases and the gradients reduce. There comes a point when for a given overall hydraulic head equilibrium is restored. The particles at the bottom will then be in limit equilibrium.

This state of limit equilibrium is the condition to fix the yet unknown head of the flow in the slit. To investigate the limiting condition two aspects must be dealt with: the interparticle forces, and the force on the particles which is exerted by the flow. In this chapter the latter is discussed. The character of the interparticle forces is investigated in chapter 8 .

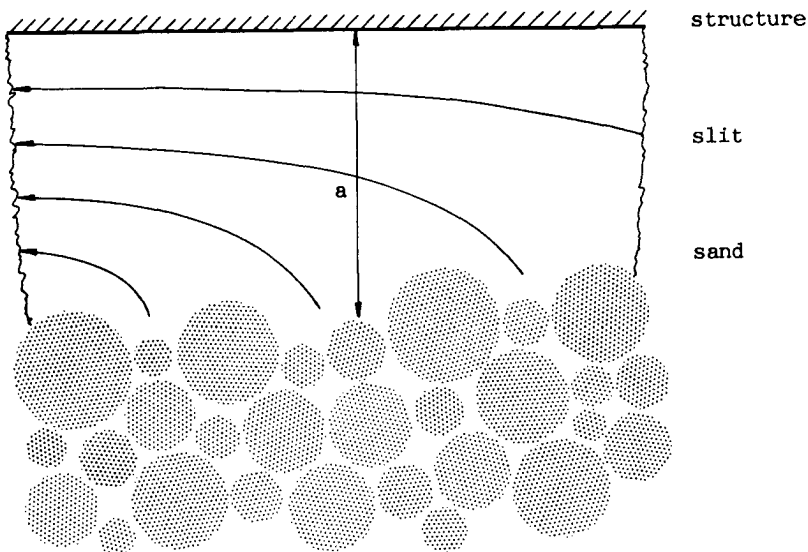


Fig. 7.1 : Flow in the slit

In figure 7.1 a detail of the geometry of the slit is shown. The depth of the slit is denoted by  $a(x)$ . The character of the flow in the slit, whether laminar or turbulent, depends on the Reynolds number. The product of average velocity and slit depth is equal to the total discharge through the slit and so the Reynolds number is  $R_e = kQ/\nu$ . Here the coefficient of permeability is denoted by  $k$ , the kinematic viscosity by  $\nu$ . If  $R_e < 600$  to  $800$  then the flow is laminar, Lamb (1945), de Vries (1979). In practice this is often true. For large permeabilities and/or large structures the number may go beyond this range. However, in this study only the laminar flow condition will be analysed.

A steady state laminar flow in general is governed by the Navier-Stokes equations, Batchelor (1983). The water velocity will be denoted by  $u$  in horizontal and  $v$  in vertical direction; the piezometric head in the slit by  $\hat{\phi}$ . If the gravitational acceleration is indicated by  $g$  and the kinematic viscosity by  $\nu$ , the Navier-Stokes equations are in case of incompressible water,

$$\begin{aligned} \left(u \frac{\partial}{\partial x} + v \frac{\partial}{\partial y}\right) u + g \frac{\partial \hat{\phi}}{\partial x} &= \nu \left(\frac{\partial^2}{\partial x^2} + \frac{\partial^2}{\partial y^2}\right) u \\ \left(u \frac{\partial}{\partial x} + v \frac{\partial}{\partial y}\right) v + g \frac{\partial \hat{\phi}}{\partial y} &= \nu \left(\frac{\partial^2}{\partial x^2} + \frac{\partial^2}{\partial y^2}\right) v \end{aligned} \quad (7.01)$$

These equations consist of a convection term, a piezometric head term and a friction term. The convection term is quadratic, the other two are linear. For small Reynolds numbers the convection term is neglected and the equations simplify to a linear system:

$$\begin{aligned} \frac{\partial \hat{\phi}}{\partial x} &= \frac{\nu}{g} \left(\frac{\partial^2}{\partial x^2} + \frac{\partial^2}{\partial y^2}\right) u \\ \frac{\partial \hat{\phi}}{\partial y} &= \frac{\nu}{g} \left(\frac{\partial^2}{\partial x^2} + \frac{\partial^2}{\partial y^2}\right) v \end{aligned} \quad (7.02)$$

As soon as  $u$  and  $v$  are determined it will be demonstrated that indeed the convection term is of minor influence. The set of two equations (7.02) contains three unknown quantities and so additional information is required. The equation of continuity must still be satisfied. In case of incompressible water it reads, Batchelor (1983),

$$\frac{\partial u}{\partial x} + \frac{\partial v}{\partial y} = 0 \quad (7.03)$$

From equations (7.02) and (7.03) the velocity and the piezometric head in the slit can be determined under the present boundary conditions. These conditions are specified in terms of the velocity. At the top of the slit the velocity vanishes; at the bottom the velocity is directed upwards and equal to  $kq$ . The depth of the slit is as yet unknown. Therefore, an extra condition is imposed, i.e. the continuity of the head,  $\hat{\phi} = P$ .

In order to solve the flow pattern in the slit fruitful use of complex calculus is made. First it is shown from equations (7.02) and (7.03) that the piezometric head is a harmonic function. This is so because differentiating the first equation of (7.02) with respect to  $x$  and the second one with respect to  $y$  leaves the Laplacean type of equation for  $\hat{\phi}$  after condition (7.03) is applied,

$$\left( \frac{\partial^2}{\partial x^2} + \frac{\partial^2}{\partial y^2} \right) \hat{\phi} = 0 \quad (7.04)$$

If the  $x,y$ -plane is now identified with the plane of the complex variable  $z$ , the harmonic function  $\hat{\phi}$  can be considered to be the real part of a complex field  $\hat{\omega} = \hat{\phi} + i\hat{\psi}$ . The real and imaginary parts of this field satisfy the Cauchy-Riemann conditions,

$$\frac{\partial \hat{\phi}}{\partial x} = \frac{\partial \hat{\psi}}{\partial y} \quad \text{and} \quad \frac{\partial \hat{\phi}}{\partial y} = - \frac{\partial \hat{\psi}}{\partial x} \quad (7.05)$$

The physical meaning of the imaginary harmonic part  $\hat{\psi}$  will appear later. The basic functions to be determined are the velocity components  $u$  and  $v$ . Since the functions  $\hat{\phi}$  and  $\hat{\psi}$  are harmonic and obey the Cauchy-Riemann conditions (7.05) the set of equations (7.02) can be rearranged into two equations of the Laplacean kind,

$$\left(\frac{\partial^2}{\partial x^2} + \frac{\partial^2}{\partial y^2}\right) \left(\frac{2v}{g} u - y \hat{\psi}\right) = 0 \quad (7.06)$$

$$\left(\frac{\partial^2}{\partial x^2} + \frac{\partial^2}{\partial y^2}\right) \left(\frac{2v}{g} v - y \hat{\phi}\right) = 0$$

There are now three equations of similar form (7.04) and the set (7.06) which can be analysed using complex calculus. In the development two only of them need to be solved, because  $\hat{\phi}$  can be expressed by the following identity, which is a consequence of (7.03) and (7.05),

$$\begin{aligned} \hat{\phi} &= \frac{\partial}{\partial y} (y \hat{\phi}) + \frac{\partial}{\partial x} (y \hat{\psi}) - \frac{2v}{g} \left(\frac{\partial u}{\partial x} + \frac{\partial v}{\partial y}\right) \\ &= -\frac{\partial}{\partial x} \left(\frac{2v}{g} u - y \hat{\psi}\right) - \frac{\partial}{\partial y} \left(\frac{2v}{g} v - y \hat{\phi}\right) \end{aligned} \quad (7.07)$$

An expression for  $\hat{\psi}$  is obtained by using (7.05), (7.06) and (7.07),

$$\begin{aligned} \frac{\partial \hat{\phi}}{\partial x} &= \frac{\partial \hat{\psi}}{\partial y} = -\frac{\partial^2}{\partial x^2} \left(\frac{2v}{g} u - y \hat{\psi}\right) - \frac{\partial^2}{\partial x \partial y} \left(\frac{2v}{g} v - y \hat{\phi}\right) \\ &= \frac{\partial^2}{\partial y^2} \left(\frac{2v}{g} u - y \hat{\psi}\right) - \frac{\partial^2}{\partial x \partial y} \left(\frac{2v}{g} v - y \hat{\phi}\right) \\ \frac{\partial \hat{\phi}}{\partial y} &= -\frac{\partial \hat{\psi}}{\partial x} = -\frac{\partial^2}{\partial x \partial y} \left(\frac{2v}{g} u - y \hat{\psi}\right) - \frac{\partial^2}{\partial y^2} \left(\frac{2v}{g} v - y \hat{\phi}\right) \\ &= -\frac{\partial^2}{\partial x \partial y} \left(\frac{2v}{g} u - y \hat{\psi}\right) + \frac{\partial^2}{\partial x^2} \left(\frac{2v}{g} v - y \hat{\phi}\right) \end{aligned}$$

Hence,

$$\hat{\psi} = \frac{\partial}{\partial y} \left( \frac{2v}{g} u - y \hat{\psi} \right) - \frac{\partial}{\partial x} \left( \frac{2v}{g} v - y \hat{\phi} \right) \quad (7.08)$$

Now the physical meaning of  $\hat{\psi}$  becomes clear. Working out equation (7.08) yields,

$$\hat{\psi} = \frac{2v}{g} \left( \frac{\partial u}{\partial y} - \frac{\partial v}{\partial x} \right) - \hat{\psi} = \frac{v}{g} \left( \frac{\partial u}{\partial y} - \frac{\partial v}{\partial x} \right)$$

So  $\hat{\psi}$  simply represents the vorticity of the flow, normalized by the parameters  $g$  and  $v$  to obtain the same dimension [m] as the head  $\hat{\phi}$ .

Generally a solution of the Laplacean may be written as the sum of complex analytical functions of the variables  $z = x + iy$  and its complex conjugate  $\bar{z} = x - iy$ . This is true, since one may write:  $\partial/\partial x = \partial/\partial z + \partial/\partial \bar{z}$  and  $\partial/\partial y = i(\partial/\partial z - \partial/\partial \bar{z})$ . By implication it follows that  $\partial^2/\partial x^2 + \partial^2/\partial y^2 = 4 \partial^2/\partial z \partial \bar{z}$ , Garabedian (1967). The sum of the two analytical functions must be such that the boundary conditions are satisfied. The ones at the bottom of the structure are easily incorporated. Here, for  $y = 0$ , the velocity vanishes so that  $u = 0$  and  $v = 0$ . This can be satisfied by subtracting two analytical functions of equal form. Bearing this in mind, the following relations are obtained, solving (7.06),

$$2v/g u = y \hat{\psi} - i \{U(z) - U(\bar{z})\} \quad (7.09)$$

$$2v/g v = y \hat{\phi} + i \{V(z) - V(\bar{z})\}$$

Here  $U$  and  $V$  are analytical functions which will be determined later on from the remaining boundary conditions. The proposed form for  $u$  and  $v$  (7.09) yields expressions for  $\hat{\phi}$  and  $\hat{\psi}$  with the aid of equations (7.07) and (7.08),



$$\hat{\phi} = V'(z) + V'(\bar{z}) + i \{U'(z) - U'(\bar{z})\} \quad (7.10)$$

$$\hat{\psi} = U'(z) + U'(\bar{z}) - i \{V'(z) - V'(\bar{z})\}$$

Both the flow equations (7.02) and the condition of continuity (7.03) as well as the boundary conditions for  $y = 0$  are now satisfied. The vorticity  $\hat{\psi}$  is no longer needed and can be disregarded. It contains no useful additional information on the head or the velocity field.

The last step of the calculation consists in fitting the boundary condition at the bottom of the slit. An exact approach is rather hard to carry out, and therefore a simplified route is taken. The following considerations are taken into account: the depth of the slit is of the order of magnitude of the particle size. The length scale of the slit is of the order of the dimensions of the structure. Therefore, if variations in the  $x$ -direction are moderate, then a first order approximation of the solution (7.09) and (7.10) is suitable for this study. The following expansions are appropriate:

$$\begin{aligned} v/g u &\approx 2 y U'(x) + y^2 V''(x) \\ v/g v &\approx -y^2 U''(x) - \frac{1}{3} y^3 V'''(x) \end{aligned} \quad (7.11)$$

$$\hat{\phi} \approx 2 V'(x)$$

In the equation for  $\hat{\phi}$  the contribution of  $U$  is negligible. This is so because  $U$  will appear to be of higher order than  $V$ . This approximated solution (7.11) allows explicit elaboration of the as yet unknown functions  $U$  and  $V$  as well as the depth of the slit  $a$ . This is achieved by applying the remaining boundary condition for  $y = -a$ , which is  $u = 0$ ,  $v = kq$  and  $\hat{\phi} = P$ , to the solution (7.11). The following result is then obtained introducing the intrinsic permeability coefficient,  $\kappa = kv/g$ , and bearing in mind that  $p = P'$ :

$$2 V'(x) = P$$

$$4 U'(x) = a p$$

(7.12)

$$4 \kappa q = -a^2 (a p)' + \frac{2}{3} a^3 p' = -\frac{1}{3} (a^3 p)'$$

The third equation is the equivalent of the condition of continuity. This condition relates the depth  $a$  to the seepage gradients  $p$  and  $q$ . In integrated form the relation will be useful later on for further calculations. Since  $q = -dQ/dx$  integration is easily performed,

$$12 \kappa Q = a^3 p \quad (7.13)$$

No integration constant appears in (7.13) because at  $x = \ell$   $a$  vanishes together with  $Q$ .

Through (7.12) the calculation of the flow in the slit is completed. While the flow pattern itself is irrelevant for the piping problem it is still interesting to see the result and the effect that the applied approximations have had on it. Using (7.11), (7.12) and (7.13) the following description of the flow field is arrived at:

$$v/g u = \frac{1}{2} p y (y+a)$$

$$v/g v = -\frac{1}{6} p' y^2 (y+a) + \kappa q (y/a)^2$$

(7.14)

$$\hat{\phi} = P$$

It is clear now why the convection term in (7.01) is not relevant. From the solution (7.14) it follows that the relative influence of this term is of the order of  $\kappa q a/v$  which is a kind of Reynolds number for the vertical velocity. This number is always small.

Obviously the shape of the solution for  $u$  and  $\hat{\phi}$  is very much like the Poisseuille solution for pipe flow (where the vertical velocity is absent). For these small values of the slit depth the vertical velocity apparently does not very much influence the structure of the horizontal velocity field and the piezometric head. It must be borne in mind, though, that  $p$  and  $a$  are variables which are controlled by equation (7.13). In the classical Poisseuille solution the values of  $p$  and  $a$  are constants, see Batchelor (1983).

For the description of the phenomenon of piping two quantities related to the flow in the slit are particularly relevant: The continuity of flow, which is adequately described by equation (7.13), and the shear stress or drag force along the bottom of the slit, which affects the particle equilibrium. The shear stress  $\hat{\tau}$  is connected to the velocity through the equation,

$$\hat{\tau} = \gamma_w \frac{v}{g} \left\{ \frac{\partial u}{\partial y} + \frac{\partial v}{\partial x} \right\} \quad (7.15)$$

From the solution (7.09) and (7.10) and applying (7.05) and the approximation (7.12) it is found that the expression for this shear stress is as follows:

$$\hat{\tau} = \gamma_w \left[ y \frac{\partial \hat{\phi}}{\partial x} + U'(\bar{z}) + U'(z) \right] \approx \gamma_w p \left( y + \frac{1}{2}a \right) \quad (7.16)$$

The drag force at the bottom follows directly by substituting  $y = -a$ . This value is to a degree an approximation for the shear exerted on the bottom because the lower boundary of the slit slopes. But the value of  $a$  increases in the  $x$ -direction so slowly that no major effect is to be expected. Finally then, the following value of the drag force denoted by  $\tau$  is found, if  $\tau = -\hat{\tau}_{y=-a}$ :

$$\tau = \gamma_w \frac{1}{2} p a \quad (7.17)$$

A similar expression for  $\tau$  is also found if the classical Poisseuille solution for pipe flow is applied. The equations for the continuity of flow (7.13) and the drag force at the bottom of the slit (7.17) will be used for further investigation of the mechanism of piping. These equations are simple in structure due to the approximation procedure applied. It is noted that more elaborate approximations are unnecessary for the conformations to hand.

## 8. Limit state equilibrium in the slit

This chapter deals with the second aspect of limiting stability as put forward at the beginning of the previous chapter: the interparticle forces. The question of limiting stability at the interface of soil and water cannot be solved by regarding the soil as a continuum. This is due to the fact that continuum mechanics allow the effective vertical stresses to vanish near the bottom of the slit. The shearing stress which is associated with the near parabolic velocity profile in the slit itself, therefore, cannot be dealt with then in a Coulomb manner. Failure phenomena due to vanishing skeleton stress need not be taken into account, since the vertical gradient is of minor importance.

To carry out single particle force balance for a grain at the top of the interface, four distinct forces must be considered. The horizontal ones are the drag force due to channel flow and the horizontal seepage gradient. The vertical ones are the weight of a particle and a force associated with the vertical seepage gradient. The condition of limiting equilibrium must be imposed; this yields a connection for the forces for a given mode of motion.

A heterogeneous mixture in steady state shows a landscape where the large grains stick out and the small ones are well buried. The treatment of the single particle stability analysis can be made arbitrarily complex by taking into account an increasing number of geometric features of the packing and variety in particle shapes. Engineering interest however must focus on a relatively simple criterion for limiting stability. An approach with three-dimensional aspects using spherical particles is offered here. The result is a rule not unlike a Coulomb criterion. At the same time the preference for the rolling mode of motion is shown while the sensitivity to a moderate selection of geometric conditions is investigated. The approach is suggested by Koenders (1987), who worked it out for two dimensions.



The general geometry of a spherical particle at the top of the soil/water interface is outlined in figure 8.1 . A top particle P is shown supported by particles in the bed. The vertical forces working on the top particle are collectively characterized by  $R_3$  and are assumed to apply in the centre of gravity. The horizontal forces are united in a force with components  $R_1$  and  $R_2$  with application point at a distance  $y$  above the centre of the grain. The supporting particles most likely are 3 or 4 in number. In limiting equilibrium, however, the force at the contact with the rear particle(s) vanishes while the contact force at the front, consisting of the resultant of the forces  $R_1$ ,  $R_2$  and  $R_3$ , is supplied by only two particles. For reasons of simplicity these supporting particles lie on the same level and the diameter of all particles is chosen equal and denoted by  $d$ .

The geometry of this assembly is characterized by the branch angles  $\alpha$  and  $\bar{\alpha}$  and the shift  $y$ . In picture 8.1.a a vertical section is presented in such a way that the supporting particles Q and R show the same projection S;  $\alpha$  is the angle between PS and the vertical. In picture 8.1.b the cross section AA of the vertical section is presented. Here,  $\bar{\alpha}$  is the angle between PQ or PR and PS.

The limit equilibrium is only satisfied if the resultant of the forces  $R_1$ ,  $R_2$  and  $R_3$  lies in the plane TUV. Therefore, the angles  $\beta$  and  $\bar{\beta}$  are introduced. In picture 8.1.c a three-dimensional view is presented of the tetrahedron TPVW, where  $\beta$  is the angle between TW and the vertical and  $\bar{\beta}$  the angle between TW and TV. The values of  $\beta$  and  $\bar{\beta}$  are related to the branch angles  $\alpha$  and  $\bar{\alpha}$  and the shift  $y$ . These relations directly follow from picture 8.1.c,

$$\begin{aligned}\tan\beta &= \sin\alpha / (\cos\alpha + 2y/d \sec\bar{\alpha}) \\ \sin\beta &= \sin\alpha \cos\bar{\alpha} / \sqrt{(\cos^2\bar{\alpha} + 4y/d \cos\alpha \cos\bar{\alpha} + 4y^2/d^2)} \\ \tan\bar{\beta} &= \sin\bar{\alpha} / \sqrt{(\cos^2\bar{\alpha} + 4y/d \cos\alpha \cos\bar{\alpha} + 4y^2/d^2)}\end{aligned}\tag{8.01}$$

The first two expressions are equivalent. They are presented since they are both used in the results obtained later.

The fact that the resultant of the forces  $R_1$ ,  $R_2$  and  $R_3$  lies within the plane TUV implies that loss of stability associated with rolling is investigated by considering equilibrium of moments. Two ways of rolling appear to be relevant. The first one is that sphere P rolls in close contact with both spheres Q and R. The other one happens when spheres P and Q have lost contact and rolling occurs with respect to another orientation. This restricts the size of the force  $R_2$ . The following two equations are associated with this,

$$\begin{aligned} R_1 &= R_2 \tan \beta \\ R_2 &\leq R_1 \csc \beta \tan \bar{\beta} \end{aligned} \quad (8.02)$$

Apart from the rolling mode, limiting equilibrium might occur in the translational mode when the normal and tangential forces at the contact points reach the interparticle friction angle  $\delta$ . If this happens, the top particle will not roll but slip backwards, keeping in touch with at least three supporting particles. The interparticle force between grains P and R is directed along TV, which makes an angle  $\epsilon$  with the normal along PV. The rolling mode will prevail if  $\epsilon \leq \delta$ . The value of  $\epsilon$  follows if applying the cosine rule in the triangle TPV of picture 8.1.c.

$$\cos \epsilon \sqrt{(1 + 4y/d \cos \alpha \cos \bar{\alpha} + 4y^2/d^2)} = 1 + 2y/d \cos \alpha \cos \bar{\alpha}$$

which is equivalent to,

$$\tan \epsilon = 2y/d \sqrt{(1 - \cos^2 \alpha \cos^2 \bar{\alpha})} / (1 + 2y/d \cos \alpha \cos \bar{\alpha})$$

Therefore, since rolling occurs if  $\epsilon \leq \delta$  or  $\tan \epsilon \leq \tan \delta$  the following condition must be satisfied,



$$\tan \delta \geq 2y/d [\sqrt{(1 - \cos^2 \alpha \cos^2 \bar{\alpha})} - \cos \alpha \cos \bar{\alpha} \tan \delta]$$

This can be rearranged to,

$$\sin \delta \geq 2y/d \sin[\arccos(\cos \alpha \cos \bar{\alpha}) - \delta] \quad (8.03)$$

This condition is always met if  $2y/d \leq \tan \delta$ . In general protruding particles show smaller values of the branch angles and the shift, while well embedded particles show the larger values. Since the sand mixture is heterogeneous, the sand-water interface never will be neatly flattened and there will always be protruding particles. That means that the onset of motion due to loss of stability of single particles will always be dominated by rolling and that (8.03) supplies information about the size of the branch angles and shift to be expected.

It has been found that the limit stability can be expressed in a Coulomb manner. Using (8.02) the sensitivity to the bedding angle is easily investigated. This angle, which is also known as the angle of repose, relates the horizontal and vertical forces on a particle and will be indicated by  $\hat{\theta}$ . If the flow angle is denoted by  $\lambda$  with  $R_2/R_1 = \tan \lambda$ , the total horizontal hydraulic force is equal to  $R_1 \sec \lambda$ . Then from (8.01) and (8.02) it follows:

$$\tan \hat{\theta} = \frac{R_1 \sec \lambda}{R_2} = \frac{\sin \alpha \sec \lambda}{\cos \alpha + 2y/d \sec \bar{\alpha}} \quad (8.04)$$

The flow angle is limited by the second equation of (8.02), because the result (8.04) is valuable only if spheres P and Q remain in contact. If  $R_2$  is beyond its critical value then an analogous approach can be set up in a different orientation, shifted roughly  $90^\circ$ , if the top particle is surrounded by 4 supporting particles. Therefore, it is sufficient to consider the appropriate values of  $\lambda$  for the current orientation.

The range of  $\lambda$  is determined by the second equation of (8.02). Using (8.01) this equation can be written as,

$$R_2 \leq R_1 \csc \alpha \tan \bar{\alpha} \quad (8.05)$$

This result appears to be independent of the parameter  $y$ . Now, the maximum flow angle  $\Lambda$  can be expressed as  $\tan \Lambda = R_2/R_1$ . Then, with the aid of (8.05) an expression is found for  $\Lambda$ ,

$$\tan \Lambda = \csc \alpha \tan \bar{\alpha} \quad (8.06)$$

In general packings are not regular and a variety of flow directions must be accounted for. It is fair to determine an averaged value of (8.06) with respect to  $\Lambda$ . This can be carried out by integration. The average value of  $\hat{\theta}$  in the range from 0 to  $\Lambda$  is defined by,

$$\tan \hat{\theta} = \frac{1}{\Lambda} \int_0^{\Lambda} \frac{\sin \alpha \sec \alpha}{\cos \alpha + 2y/d \sec \bar{\alpha}} d\Lambda \quad (8.07)$$

The integral is a standard one to be found for instance in Gröbner and Hofreiter (1975) part I, 331, 9c. The result of integration is,

$$\tan \hat{\theta} = \frac{1}{\Lambda} \frac{\sin \alpha \operatorname{arctanh}(\sin \Lambda)}{\cos \alpha + 2y/d \sec \bar{\alpha}} \quad (8.08)$$

This expression yields not yet the global average bedding angle. As mentioned before there are four orientations. The true average is therefore determined by:  $\sum \Lambda \tan \hat{\theta} / \sum \Lambda$ , where the  $\sum$  sign indicates summation over the four orientations and  $\sum \Lambda = \pi$ . The average bedding angle becomes then,

$$\tan \hat{\theta} = \frac{1}{\pi} \sum_{n=1}^4 \frac{\sin \alpha_n \operatorname{arctanh}(\sin \Lambda_n)}{\cos \alpha_n + 2y/d \sec \bar{\alpha}_n} \quad (8.09)$$

Quite a few geometric features of the packing are involved in this stage. As mentioned in the beginning of this chapter the goal is to obtain a reliable but simple criterion for the limiting

stability. Therefore, a simplification will be put forward. Right now the supporting particles form a quadrangle. If they form a rectangle, however, symmetry is obtained between orientations 1 and 3 and between 2 and 4 so that  $\Lambda_1 + \Lambda_2 = \frac{1}{2}\pi$ . Moreover, from picture 8.1.c it can be seen that the length of OW in orientation 1 is equal to the one of VW in orientation 2 and vice versa. This implies that,

$$\begin{aligned} \sin\alpha_1 \cos\bar{\alpha}_1 &= \sin\bar{\alpha}_2 \\ \sin\alpha_2 \cos\bar{\alpha}_2 &= \sin\bar{\alpha}_1 \end{aligned} \quad (8.10)$$

These conditions, substituted in equation (8.06), indeed imply that  $\Lambda_1 + \Lambda_2 = \frac{1}{2}\pi$ .

Meanwhile, the bedding angle can be written as,

$$\tan\hat{\theta} = \frac{2}{\pi} \left[ \frac{\sin\alpha_1 \operatorname{arctanh}(\sin\Lambda_1)}{\cos\alpha_1 + 2y/d \sec\bar{\alpha}_1} + \frac{\sin\alpha_2 \operatorname{arctanh}(\sin\Lambda_2)}{\cos\alpha_2 + 2y/d \sec\bar{\alpha}_2} \right] \quad (8.11)$$

It is convenient to express the items with index 2 into items with index 1. The set (8.10) can be rearranged with use of (8.06) to,

$$\begin{aligned} \sin\alpha_2 \cos\bar{\alpha}_2 &= \sin\alpha_1 \cos\bar{\alpha}_1 \tan\Lambda_1 \\ \cos\alpha_2 \cos\bar{\alpha}_2 &= \cos\alpha_1 \cos\bar{\alpha}_1 \end{aligned} \quad (8.12)$$

From picture 8.1.c it may be noticed that the first equation concerns the quotient of VW and OW in orientations 1 and 2. The second one says that OP in both orientations must be equal. The bedding angle (8.11) now can be expressed in the index 1 only, keeping in mind that  $\Lambda_1 + \Lambda_2 = \frac{1}{2}\pi$ ,

$$\tan\hat{\theta} = \frac{\sin\alpha [\operatorname{arctanh}(\sin\Lambda) + \tan\Lambda \operatorname{arctanh}(\cos\Lambda)]}{\frac{1}{2}\pi (\cos\alpha + 2y/d \sec\bar{\alpha})} \quad (8.13)$$

Since from now on only one orientation is concerned, there is no need anymore for an index. The ultimate result of the bedding angle is obtained by combining (8.13) with (8.06) into,

$$\tan \hat{\theta} = \frac{\sin \alpha \operatorname{arcsinh}(\tan \bar{\alpha} / \sin \alpha) + \tan \bar{\alpha} \operatorname{arcsinh}(\sin \alpha / \tan \bar{\alpha})}{\frac{1}{2} \pi (\cos \alpha + 2y/d \sec \bar{\alpha})} \quad (8.14)$$

The smaller branch angles indicate the more protruding particles, while larger ones correspond to well embedded grains. A word must be said about the values of the branch angles to be expected. The smallest value  $\bar{\alpha}$  may have is  $30^\circ$ . A maximum value is likely to be  $60^\circ$ , when the top particle is half embedded between the supporting particles. The value of  $\alpha$  may lie in theory anywhere between  $0^\circ$  and  $90^\circ$ . However, particles with an angle in the range from  $0^\circ$  to  $45^\circ$  are relatively weak and easily moved away. Particles, resisting the flow will have typically an angle in the order of  $45^\circ$  to  $75^\circ$ . For angles beyond, there is no clear distinction anymore between top and supporting particles.

The shift  $y$  is not an arbitrary parameter but depends rather on the current sizes of  $\alpha$  and  $\bar{\alpha}$ . Its value will decrease when the branch angles become smaller and vice versa. It is quite difficult to derive a relation, but some qualitative aspects may be stated. It is obvious that the position of the crest of the supporting particles controls to what extent the free water flow penetrates. This position with respect to the centre of the top particle is equal to  $\frac{1}{2}d - d \cos \alpha \cos \bar{\alpha}$ . If this quantity is negative, what means that the crest of the supporting particles lies below the centre of the top particle, then the value of  $y$  virtually will vanish. But if all particles are well embedded, which is the case for  $\alpha = 90^\circ$ , then the top half of all the particles is in close contact with the free water, leading to values of  $y$  equal to approximately  $\frac{1}{2}d$ . Therefore, as a rough estimate of the shift  $y$  the following is proposed,

$$2y/d = \frac{1}{2} - \cos \bar{\alpha} \cos \alpha \quad \frac{1}{2} \geq \cos \alpha \cos \bar{\alpha} \quad (8.15)$$

$$2y/d = 0 \quad \frac{1}{2} < \cos \alpha \cos \bar{\alpha}$$

Now it is the right moment to check the condition of the rolling mode (8.03). Together with (8.15) this may be written,

$$\sin \delta \geq (\frac{1}{2} - \cos \alpha \cos \bar{\alpha}) \sin[\arccos(\cos \alpha \cos \bar{\alpha}) - \delta] \quad (8.16)$$

It appears that there is a minimum value of  $\cos \alpha \cos \bar{\alpha}$ , depending on the interparticle friction angle, beyond which rolling fails due to slip between the particles. Rowe (1962) suggests values of the friction angle in the order of  $20^\circ$ , arriving at a minimum size of about 0.12 for  $\cos \alpha \cos \bar{\alpha}$ . This matches very well the afore considered range of the branch angles.

The relation (8.14) combined with (8.15) presents a description of the bedding angle as function of the branch angles. Figure 8.2

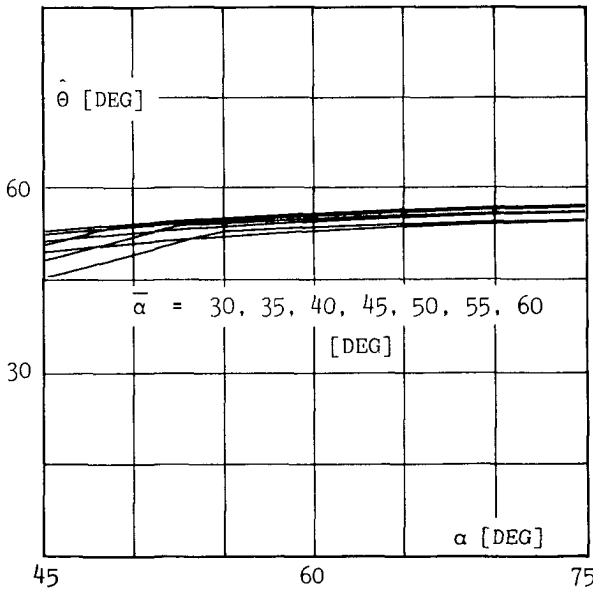


Fig. 8.2 : Relation between bedding angle and branch angles

shows the result for various values of  $\alpha$  and  $\bar{\alpha}$ , leaving a relatively sharp criterion for  $\tan \hat{\theta}$  with  $\hat{\theta}$  in the range of  $50^\circ$  to  $55^\circ$ . Similar values are reported in the literature by experimentalists, Fernandez Luque and Van Beek (1976), White (1940). For non-spherical particles higher bedding angles are to be expected.

The relation (8.14) is only valuable for a top particle at the interface of soil and water. The behaviour of particles well within the bed is presented in various papers. A result found by Dantu (1961) as well as Rowe (1962) is,

$$\sin \hat{\theta} = \frac{1}{3} + \frac{1}{3}\sqrt{3} \tan \delta \quad (8.17)$$

Here, the interparticle friction plays a role due to translational motion rather than a rolling one. Though this formula has no relation to the result (8.14), the value of the bedding angle shows the same order of magnitude, since  $\delta \approx 20^\circ$ .

The horizontal drag is a generalized shear force per unit area. The drag per particle depends on the amount of grains per unit area. Therefore, a factor  $\hat{C}$  is introduced, called drag factor and defined as the ratio of influenced area and particle cross section. Its value depends very much on the particle distribution and the density of the top layer. During the erosion process the smaller particles are easily transferred, while the larger ones resist the flow. White (1940) has performed experimental research on the equilibrium of grains on a stream bed. He found that the factor  $\hat{C}$  ranged from 3 to 4. Roughly these values correspond to an amount of 65% to 75% smaller grains. For the diameter  $d$  therefore a value between  $d_1$  and  $d_2$  must be chosen.

An elegant and simple criterion for the ratio of horizontal and vertical force on a particle is defined now. Besides, the actual drag factor of the shearing force on a particle is specified. What is left to be done is the further articulation of the forces itself. The following forces play a role in the failure criterion: the drag force, the seepage gradient and the unit weight of

particles. In the horizontal direction the drag is defined by equation (7.17); the component of the gradient by  $p$ . The gradient gives a result similar to the buoyancy of a particle in a fluid. The drag per particle has already been discussed, introducing the drag factor  $\hat{C}$ . The resulting horizontal force per unit volume and per unit weight of water is then  $p \hat{C} a/d + p$ . The unit volume concerned is the volume of a sphere,  $\pi/6 d^3$ .

In the vertical direction two buoyancy type forces act: the gradient and the submerged weight of particles. Therefore, the vertical force per unit volume and per unit weight of water is likely to be  $\gamma_p'/\gamma_w - q$ , where  $\gamma_p'$  indicates the submerged unit weight of particles. However, Martin (1970) has discovered that the seepage force on the interfacial grains differs from the one on grains well within the bed. The reason is that the pressure gradient collapses across the top particles. Consequently, the seepage force on a top particle is lower than the assumed value of  $q$ . Martin introduces a factor  $C$ , called here surface factor, by which  $q$  must be multiplied in order to obtain a realistic seepage force. Values of  $C$  ranging from 0.35 to 0.50 are determined.

The ratio of the horizontal to the vertical force on a top particle is equal to  $\tan \hat{\theta}$ . This leads to the following condition,

$$C q + p (\hat{C} a/d + 1) \cot \hat{\theta} = \gamma_p'/\gamma_w \quad (8.18)$$

Here,  $a$  is defined by equation (7.13),

$$p a^3 = 12 \kappa Q \quad (8.19)$$

Relation (8.18) together with (8.19) serves to select a particular solution for the flow in the slit, just as equation (6.05) does for the sandboil.

## 9. Evaluation

In the previous chapters elements of the analysis of piping under a geotechnical structure have been studied. These are now put together. First a short review of the intermediate results is given. The starting point is the condition of limit equilibrium in the sandboil represented by equation (6.05),

$$\gamma_w / \gamma_s q + p/q \cot \theta = 1 \quad (9.01)$$

In the slit, similarly limiting equilibrium and continuity of flow are expressed by relations (8.18) and (8.19),

$$C q + p (\hat{C} a/d + 1) \cot \theta = \gamma_w / \gamma_p \quad (9.02)$$

$$p a^3 = 12 \kappa Q$$

In these equations the horizontal and vertical gradients,  $p$  and  $q$ , as well as the head  $P$  and the flow function  $Q$  are related to each other. The groundwater flow problem as solved in chapter 5 may still assume a great variety of forms depending on the choice of the coefficient  $A_n$  in equations (5.11) and (5.13). Specifically for  $0 < x < \ell$  these equations are,

$$p = \frac{dP}{dx} = \sum_{n=0}^{\infty} A_n \sin\{(n+\frac{1}{2}) \pi \xi\} \quad (9.03)$$

$$q = \frac{1}{\pi} \int_0^{\ell} \frac{dP}{dr} \sqrt{\frac{\ell-x}{\ell-r}} \frac{dr}{r-x} = \sum_{n=0}^{\infty} A_n \cos\{(n+\frac{1}{2}) \pi \xi\}$$



$$P = \sum_{n=0}^{\infty} A_n \frac{\ell}{4} \left[ \frac{\sin\{(n-\frac{1}{2}) \pi \xi\}}{(n-\frac{1}{2})} - \frac{\sin\{(n+\frac{1}{2}) \pi \xi\}}{(n+\frac{1}{2})} \right] \quad (9.04)$$

$$\begin{aligned} -Q &= \sum_{n=0}^{\infty} A_n \frac{\ell}{4} \left[ \frac{\cos\{(n-\frac{1}{2}) \pi \xi\}}{(n-\frac{1}{2})} - \frac{\cos\{(n+\frac{1}{2}) \pi \xi\}}{(n+\frac{1}{2})} \right] \\ &= \frac{1}{\pi} \int_0^{\ell} P \sqrt{\left(\frac{\ell-x}{\ell-r}\right)} \frac{dr}{r-x} - \frac{2}{\pi} \int_0^{\ell} \sqrt{(\ell-x)} \int_0^{\ell} \frac{dP}{dr} \frac{dr}{\sqrt{(\ell-r)}} \end{aligned}$$

Here, the transformed value  $\xi$  is copied from (5.12),

$$\xi = 2/\pi \arcsin \sqrt{x/\ell} \quad (9.05)$$

Alternatively instead of giving a set for the  $A_n$  an influence function  $p$  may be prescribed. In so doing an integral type solution is sought rather than expressing the result in terms of Fourier series. It must be stressed that the two alternative solutions are entirely equivalent. Conditions (9.01) and (9.02) are employed to force (9.03) and (9.04) into a solution.

For the calculation it is essential to know the size of the sandboil and the slit. It is realistic to suppose that the amount of sand transferred from the slit is equal to that transferred to the sandboil. If one ignores the fact that the density of the sand has changed then a fair assumption is that the volumes of sandboil and slit are equal. A first order value of the height of the sandboil follows from (5.19),  $h \approx P/q$ . Therefore, the width  $b$  of the sandboil is determined by,

$$\int_0^b \frac{P}{q} dx = \int_b^{\ell} a dx \quad (9.06)$$

The value of the erosion length  $\ell$  is related to the applied hydraulic head  $H$  across the structure. For reasons of simplicity the hydraulic head will be considered to be the value of the head

along the structure at a certain distance  $x = L$ , with  $L > \ell$ . The value of  $L$  corresponds to the length of the structure plus the length of the sandboil. Since the sandboil is much smaller than the structure,  $L$  is roughly the length of the structure. The results are slightly influenced by the fact that there is no real free surface at  $x = L$  but rather a gradually increasing head. To understand the mechanism of piping this is not important.

The head along the structure is introduced in equation (5.15). Here, the value of  $n$  is given in (5.14). Substitution of  $\Phi = H$  and  $x = L$  leads to the following condition,

$$H = \sum_{n=0}^{\infty} (-1)^n A_n \frac{\ell}{4} \left[ \frac{\exp\left\{\left(n+\frac{1}{2}\right) \pi n\right\}}{\left(n+\frac{1}{2}\right)} - \frac{\exp\left\{\left(n-\frac{1}{2}\right) \pi n\right\}}{\left(n-\frac{1}{2}\right)} \right] \quad (9.07)$$

$$= -\frac{1}{\pi} \int_0^{\ell} p \sqrt{\left(\frac{L-\ell}{\ell-r}\right)} \frac{dr}{r-L} + \frac{2}{\pi} \sqrt{(L-\ell)} \int_0^{\ell} \frac{dp}{dr} \frac{dr}{\sqrt{(\ell-r)}}$$

where,

$$\exp\left(-\frac{1}{2} \pi n\right) = \sqrt{(L/\ell)} + \sqrt{(L/\ell - 1)} \quad L > \ell \quad (9.08)$$

Through the system (9.01) ... (9.08) the as yet unknown influence function  $p$  or alternatively the coefficients  $A_n$  can be determined. Note that because of (9.07) the hydraulic head  $H$  cannot exceed a critical value. This will be elucidated later on.

The general nature of the solution is investigated before proceeding to a large-scale numerical elaboration. If one considers dimensionless quantities it appears that, generally speaking, a relation between  $H/L$  and  $\ell/L$  is put forward for a given set of parameters. This relation is written in shorthand as follows:

$$\frac{H}{L} = \frac{H}{L} \left[ \frac{\ell}{L} ; \hat{C} \left( \frac{\kappa L}{d^2} \right)^{\frac{1}{2}}, \frac{\gamma_p}{\gamma_w} \tan \hat{\theta}, C \tan \hat{\theta}, \frac{d}{L}, \theta, e \right] \quad (9.09)$$

where,  $1+e = \gamma_p^*/\gamma_s^*$ ;  $e$  is the void ratio. The way the soil parameters appear in the formula is such that only certain clusters need to be considered. But from an engineering point of view it is convenient to specify the parameters by their physical relevance. Therefore, the following relation is suggested,

$$\frac{H}{L} = \frac{H}{L} \left[ \frac{\ell}{L} ; \frac{\kappa}{d^2} , \frac{d}{L} , C , \hat{C} , \theta , \hat{\theta} , \frac{\gamma_p^*}{\gamma_w} , e \right] \quad (9.10)$$

The results will be plotted in the following manner:  $H/L$  on the ordinate and  $\ell/L$  on the abscissa. A curve is defined for each combination of parameters after the semi-colon in formula (9.10).

In order to compute relations (9.10) a computer program has been written. As a first trial the procedure of collocation has been chosen employing the Fourier expansion of the solution. The result turned out to contain very unpleasant oscillations, most probably due to the abrupt transitions on the boundaries. Another numerical scheme based on descriptions of the integral representation of the solution suffered a similar fate.

Obviously a method like collocation used without further precautions is insufficient to deal with sharp transitions such as may occur at the boundaries. Therefore, a different or at least a modified procedure should be followed. Broken off Fourier expansions are a strong tool if the coefficients can be obtained by integration. If the collocational principle can be replaced by a variational principle, the broken off Fourier series becomes much more attractive. There is, however, the difficulty that the variational approach has a non-linear character and therefore this approach is better avoided.

A modified numerical procedure is now outlined. It must be borne in mind that a description by Fourier series is general and arbitrary shapes can be handled. Wild curves are to be expected in the transition zones. The solution relies on the implementation of adapted shape functions in the computer program. A more thorough investigation of the solution in the transition zones is needed.

This is carried out in appendix A . In appendix B a full implementation is shown for all three transition zones. It is inconvenient to determine the special shape functions from the Fourier representation of the problem. Rather they are obtained from the integral form.

In the appendices it is demonstrated that the abrupt behaviour is well captured by hypergeometric shape functions. Such functions can deal with any continuous characteristics. They are readily implemented in a numerical scheme. As was to be expected the oscillations disappear and a physically realistic result is obtained. In Sellmeijer (1986) the influence of hypergeometric shape functions is demonstrated under simplified conditions.

The task of describing the mechanism of piping is now completed. The results may be evaluated. For a good overall picture it is sufficient to show three distinct cases: a massive dike with a length of 80 m ; a small dam with a length of 8.0 m ; and a laboratory test model of length 0.80 m . The soil parameters chosen in all three cases are equal to those assessed by De Wit et al. (1981) during their laboratory tests.

Figure 9.1 shows the computed relations between  $H/L$  and  $\ell/L$  . It can be clearly seen that a critical value of  $H$  exists. Beyond that, equilibrium cannot be reached. To the left of the critical  $H$  the erosion length  $\ell$  is stable. Here a fluctuation in  $H$  is compensated for by a small increase in  $\ell$  . But to the right of the critical head a variation in  $\ell$  demands a subsequent decrease of  $H$  . If the hydraulic head stays constant a progressive process of erosion is set in motion, resulting in the total collapse of the dike. This behaviour - a stable situation followed by progressive erosion at full swing - exactly coincides with observations in practice.

This qualitative outcome is encouraging, but the real interest is how the theoretical result relates to the measurements of the laboratory model tests of De Wit et al. (1981) . Model tests were performed in a container, where the outflow region was similar to

$$\begin{aligned} \kappa/d^2 &= 0.0005 & \gamma_p/\gamma_w &= 1.65 & \theta &= 36^\circ & c &= 0.4 \\ e &= 0.80 & \hat{\theta} &= 54^\circ & \hat{c} &= 4.0 \end{aligned}$$

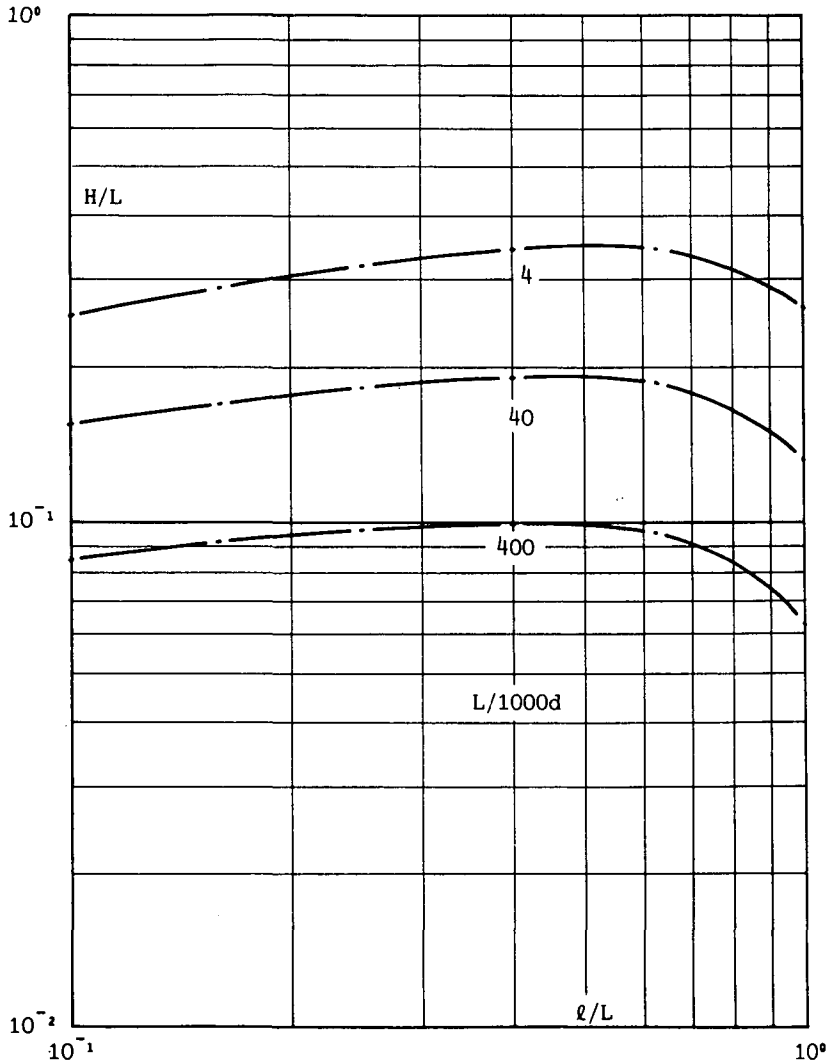


Fig. 9.1 : Relation between  $H/L$  and  $l/L$

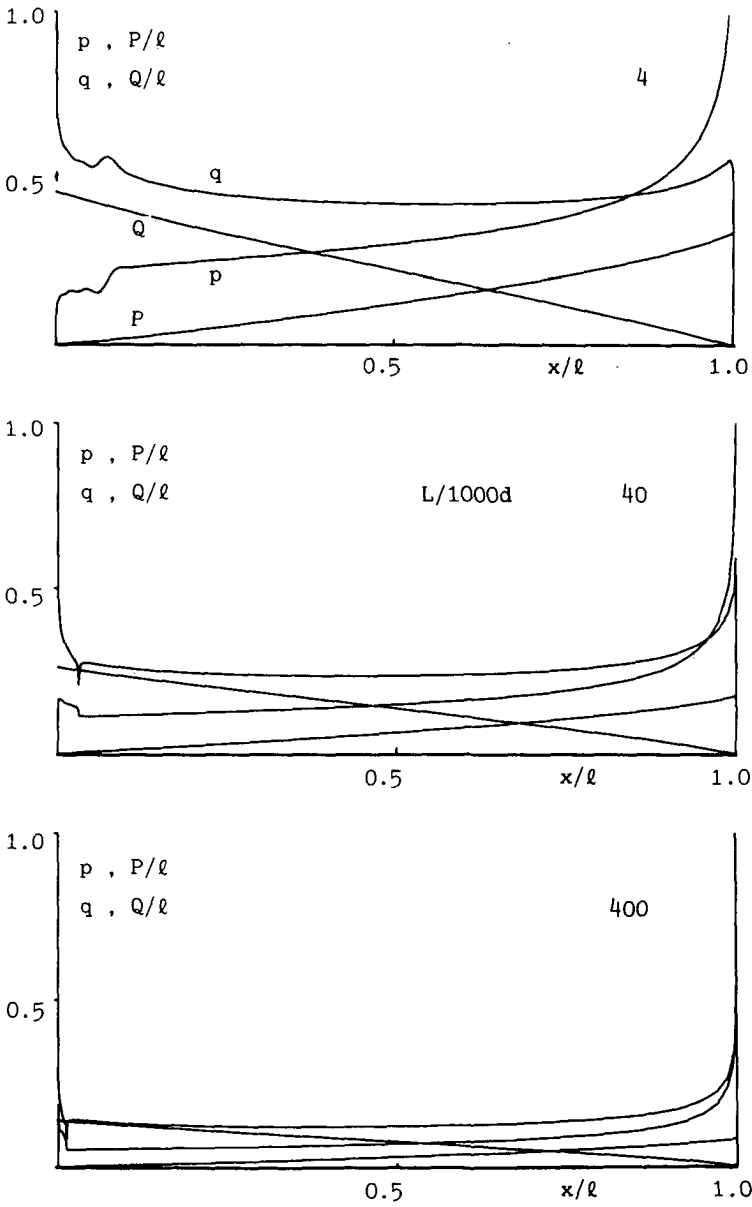


Fig. 9.2 : Distributions of  $p$ ,  $P$ ,  $q$  and  $Q$  for  $\ell/L = 0.4$

that in figure 4.1 . The dike length was varied from 0.80 m to 2.40 m and three types of sand were used. The tests were repeated several times. Most of the tests were performed with river sand for a dike length of 0.80 m with the measured critical head ranging from 0.25 to 0.35 m . The result of the calculation is 0.28 m . Measurements and calculations for the other types of sand show the same tendency. The agreement is excellent.

So much for the small container tests. The large tests need some explanation. There the development of the sandboils was unintentionally restricted because of the way in which the test was designed. The sandboil plays a somewhat ambivalent but crucial role. It must exist in order to ensure that water can be released from the slit, and once it is allowed to arise freely its properties do not influence the critical head significantly. When the sandboil's development was restricted as in the above mentioned large tests, the measurements hardly exceeded those obtained in the small container tests. Therefore the results of these large tests are of no use in checking the model under study.

Figure 9.2 shows some intermediate results of  $p$  ,  $P$  ,  $q$  and  $Q$  . It can be noticed that these graphs show a rather abrupt transition behaviour. But due to the stable numerical procedure hardly any oscillations occur. A last word must be said about the accuracy of the calculation procedure. The conditions (9.01) and (9.02) are satisfied to a high degree, but the solution appears to have some flexibility in the relation between  $p$  and  $q$  . A variation in  $p$  upwards is easily compensated for by a smaller value for  $q$  and vice versa. This is due to the tendency to flatten down the transitions for a limited number of shape functions. There is hardly a global influence but it helps suppressing oscillations resulting in an ultimate accuracy of the order of 1% in the equilibrium conditions. This figure is not of great significance in the results.

## 10. Design formula

In the previous chapters a criterion for the appearance of piping is successfully derived. This criterion is the critical hydraulic head which can appear across the geotechnical structure. A computer code is defined in order to determine this critical item. Examples of calculation are shown in figure 9.1. The computer program is very useful to obtain quantitative results, but the code of the solution is not yet clear enough to understand the structure of the results. Moreover, a tractable engineering tool is preferred in order to design dikes and dams in practice.

It is possible to obtain qualitative insight into the solution by approximation. The result will turn out to be a reliable condition for the appearance of piping. To achieve this the following starting points are taken into account:

- i ) From the results of the calculations it is seen that the influence exerted by the parameters of the sandboil is minimal, though its presence is vital. As an approximation the function of the sandboil may be simulated by a value  $p \neq 0$  in  $x = 0$ , determined by the condition in the slit. As a consequence the value of  $q$  will then show a logarithmic singular behaviour in  $x = 0$ . It must be checked if this adversely affects results.
- ii ) The condition (9.02) contains the value of  $q$ . It appears from figure 9.2 that  $q$  is rather constant except for the very beginning and end values. As an approximation  $q$  may be replaced by the averaged value in the range of  $x$  between 0 and  $l$ . Thus the logarithmic singularity in  $x = 0$  plays no role.
- iii) The behaviour of  $p$  will be estimated from the results of figure 9.2. Attention is paid to the shapes of  $p$  and  $Q$ , and the value of  $Q/p$  in  $x = 0$ . It is known that  $p$  and



$Q$  are related to each other by condition (9.02) and equation (9.04).

In i) and ii) the condition (9.02) is made valid in the entire interval  $0 - \ell$ . This condition is written as follows:

$$p \{ \frac{1}{2} \hat{C} (12 \kappa / d^2 Q / p d)^{\frac{1}{2}} + 1 \} = (\gamma_p / \gamma_w - C Q_0 / \ell) \tan \hat{\theta} \quad (10.01)$$

where the vertical gradient  $q$  is replaced by the average vertical gradient  $Q_0 / \ell$ , if  $Q_0$  is the value of  $Q$  for  $x = 0$ . It is seen from this equation that the clusters of parameters coincide with the ones in (9.09). At first the relation (10.01) between  $p$  and  $Q$  will be worked out. Thereto, a normalized quantity like the following is introduced,

$$\hat{f} = f / \{ c (\gamma_p / \gamma_w - C Q_0 / \ell) \tan \hat{\theta} \} \quad (10.02)$$

Here  $f$  may be replaced by either  $p$ ,  $P$ ,  $q$ ,  $Q$  or  $H$ . The parameter  $c$  is defined as,

$$c = \frac{1}{2} \hat{C} (12 \kappa / d^2 Q_0)^{\frac{1}{2}} \quad (10.03)$$

Accordingly, the condition (10.01) simplifies to,

$$(Q/Q_0 1/p)^{\frac{1}{2}} + c = 1/p \quad (10.04)$$

In general the value of  $c$  tends to be much smaller than unity and therefore the relation (10.04) may be approximately written,

$$1/p = (Q/Q_0)^{\frac{1}{2}} + c \quad (10.05)$$

This parabolic result may be substituted into the second relation of (9.04) normalized by (10.02). Thus  $p$  and  $Q$  are defined, but the solution of the integral equation is cumbersome. Therefore an alternative method will be followed, indicated in iii). The

shape of the horizontal gradient and the total discharge will be estimated from the computed results. The graphs of figure 9.2 show that the following approach will do well:

$$p = 1 / \{(1-x)^\beta + c\} \quad Q/Q_0 = (1-x)^{2\beta} \quad (10.06)$$

Here  $\beta$  is a parameter which will be used to adjust this approach as close as possible to the results of calculation. Note that the relation (10.05) is satisfied.

Now the stage is set for an approximation formula. What has to be done is to find out if the above estimation fits the physics of the phenomenon of piping - in other words, if the assumption (10.06) meets within reasonable limits the second relation of (9.04). Investigating this, the value of  $\beta$  is determined and that of  $Q_0$  will follow.

The procedure is to substitute the assumed values of (10.06) into the second equation of (9.04). Thereto one also needs the variable  $P$  which can be obtained by integration of  $p$  with respect to  $x$  since  $p = dP/dx$ . The details of the elaboration are to be found in appendix C. Making use of (C.03) the second equation of (9.04) can be written with the aid of (10.02) and (10.06),

$$\begin{aligned} \frac{Q_0}{l} (1-x)^{2\beta} &= - \frac{2}{\pi} \int_0^1 \frac{1}{(1-\rho)^\beta + c} \sqrt{\frac{1-x}{1-\rho}} d\rho - \\ &- \frac{1}{\pi} \int_0^1 \left\{ \frac{1 - (1-\rho)^{1-\beta}}{1-\beta} - c \frac{1 - (1-\rho)^{1-2\beta}}{1-2\beta} \right\} \sqrt{\frac{1-x}{1-\rho}} \frac{d\rho}{\rho-x} \end{aligned} \quad \beta < \frac{1}{2} \quad (10.07)$$

The integration variable here is made dimensionless. Now a value of  $\beta$  must be determined such that the equation (10.07) is met within reasonable limits. It will turn out that the value of  $\beta$  will be about 0.4. Therefore both sides of the equation must show a more or less straight behaviour, which is to be expected.

To work this out is quite troublesome and does not seem to be a very strict condition. Much better is the following approach. The ratio of  $Q/\ell p$  at the beginning of the slit is according to the results of figure 9.2 well defined and the approximation must reflect this to a reasonable extent. The ratio  $Q/\ell p$  of the approximation at  $x = 0$  is equal to  $(1+c) Q_0/\ell$  what results from (10.02) and (10.06). Therefore the value of  $\beta$  will be determined callibrating the calculated values of  $Q_0/\ell$  from equation (10.07) for  $x = 0$  with the results of figure 9.2 ,

$$\frac{Q_0}{\ell} = \frac{2}{\pi} \int_0^1 \frac{1}{(1-\rho)^\beta + c} \sqrt{\frac{1}{1-\rho}} d\rho - \quad \beta < \frac{1}{2} \quad (10.08)$$

$$- \frac{1}{\pi} \int_0^1 \left\{ \frac{1 - (1-\rho)^{1-\beta}}{1-\beta} - c \frac{1 - (1-\rho)^{1-2\beta}}{1-2\beta} \right\} \frac{1}{\rho} \frac{d\rho}{\sqrt{(1-\rho)}}$$

It is possible to work out the integration in a closed form. The details of the procedure are given in appendix C . The result is expressed by equation (C.20),

$$\begin{aligned} \frac{Q_0}{\ell} = & \frac{4}{\pi} \left[ \frac{1}{1-2\beta} + c^{\frac{1}{2\beta}-1} \frac{\pi}{2\beta} \csc\left(\frac{\pi}{2\beta}\right) + \frac{c}{4\beta-1} \right] - \\ & - \frac{1}{\pi} \left[ \frac{\Psi(\frac{1}{2}-\beta) - \Psi(\frac{1}{2})}{1-\beta} - c \frac{\Psi(\frac{1}{2}-2\beta) - \Psi(\frac{1}{2})}{1-2\beta} \right] \end{aligned} \quad \frac{1}{2} < \beta < \frac{1}{2} \quad (10.09)$$

Here,  $\Psi$  is the so-called psi-function. Careful fitting of the calculated  $Q_0/\ell$  values at last leads to the following value of  $\beta$  ,

$$\beta = 0.37 (1+c) \quad (10.10)$$

The values of  $\beta$  are limited to the range  $\frac{1}{2} < \beta < \frac{1}{2}$  due to the followed procedure to derive (10.09).

An important result is reached now. A well chosen shape of the horizontal gradient is determined. It consists of (10.06) together with (10.02), (10.03), (10.09) and (10.10). The final step of the procedure will be the determination of the critical head defined by (9.07). This equation supplies a range of values for  $H/L$  as function of  $\ell/L$  from which the maximum possible one must be calculated in order to obtain the critical head. One may observe in figure 9.1 that the desired maximum value is fairly well represented by the head for  $\ell = \frac{1}{2}L$ . Therefore the critical head will be defined as that for  $\ell = \frac{1}{2}L$ . Thus using the integral representation (9.07) and the relations (10.06) and (C.03) the following is obtained,

$$\begin{aligned} \frac{H(\frac{1}{2}L)}{L} &= \frac{1}{\pi} \int_0^1 \frac{1}{(1-\rho)^\beta + c} \sqrt{\frac{1}{1-\rho}} d\rho + \\ &+ \frac{1}{2\pi} \int_0^1 \left\{ \frac{1 - (1-\rho)^{1-\beta}}{1-\beta} - c \frac{1 - (1-\rho)^{1-2\beta}}{1-2\beta} \right\} \frac{1}{2-\rho} \frac{d\rho}{\sqrt{(1-\rho)}} \end{aligned} \quad \beta < \frac{1}{2} \quad (10.11)$$

Again the details of integration are in appendix C. The result follows from (C.24),

$$\frac{H(\frac{1}{2}L)}{L} = \frac{Q_0}{\frac{1}{2}L} + \frac{1}{2\pi} \left[ \frac{\Psi(\frac{1}{2}-\frac{1}{2}\beta) - \Psi(\frac{1}{2})}{1-\beta} - c \frac{\Psi(\frac{1}{2}-\beta) - \Psi(\frac{1}{2})}{1-2\beta} \right] \quad (10.12)$$

Here too, the values of  $\beta$  are limited to the range  $\frac{1}{2} < \beta < 1$ . The expression (10.12) is determined with the aid of equations (10.02), (10.03), (10.09) and (10.10). These are summarized once again here, still with the general notation  $\ell$ . If applied to (10.12)  $\ell$  has to be replaced by  $\frac{1}{2}L$ . The normalization formula (10.02) is inverted.

$$\frac{Q_0}{\ell} = \frac{4}{\pi} \left[ \frac{1}{1-2\beta} + c^{\frac{1}{2\beta}-1} \frac{\pi}{2\beta} \csc\left(\frac{\pi}{2\beta}\right) + \frac{c}{4\beta-1} \right] -$$

$$- \frac{1}{\pi} \left[ \frac{\Psi\left(\frac{1}{2}-\beta\right) - \Psi\left(\frac{1}{2}\right)}{1-\beta} - c \frac{\Psi\left(\frac{1}{2}-2\beta\right) - \Psi\left(\frac{1}{2}\right)}{1-2\beta} \right] \quad (10.13)$$

$$\beta = 0.37 (1+c) \quad (10.14)$$

$$c = \frac{1}{2} \hat{C} \left( \frac{1}{1+\beta} d^2 / \kappa d / \ell \right)^{\frac{1}{2}} / (Q_0 / \ell)^{\frac{1}{2}} \quad (10.15)$$

$$f = f_c \gamma_p' / \gamma_w \tan \hat{\theta} \left[ 1 - 1 / \left\{ 1 + 1 / \left[ C Q_0 / \ell c \tan \hat{\theta} \right] \right\} \right] \quad (10.16)$$

Here,  $f$  stands for  $H$  or  $Q$ .

Only for reasons of comparison, the value of the hydraulic head for  $\ell = L$  is joined. This value is already determined in appendix C in (C.08),

$$\frac{H(L)}{L} = \frac{1}{1-\beta} - \frac{c}{1-2\beta} - \frac{c^2}{3\beta-1} + c^{\frac{1}{\beta}-1} \frac{\pi}{\beta} \csc\left(\frac{\pi}{\beta}\right) \quad (10.17)$$

In this formula the values of  $\beta$  must lie in the range  $\frac{1}{2} < \beta < \frac{3}{2}$ . The set (10.13) ... (10.16) which is used to determine (10.12) must also be applied to work out (10.17). However, then  $\ell$  must be replaced by  $L$ .

A relatively simple estimation of the critical head is found now. The intriguing question is how accurate these formulae (10.12) and (10.17) can predict piping. Therefore calculations are performed for the three cases studied in chapter 9. A remarkable agreement is obtained. The accuracy is better than 3 %.

Up till now a cautious and precise procedure is followed to obtain a very reliable approximate description of the piping phenomenon. One might put forward that a less accurate way could have been followed resulting in a more severe, but less accurate result. It

is believed that this would be a mistake, because the mechanism of piping is rather complicated and must be treated with care. However, the present approximation (10.12) is quite appropriate to investigate the structure of the solution. It will appear that using the technique of curve fitting this result can be represented by a most elegant and short formula.

It is observed from (10.12) ... (10.17) that three clusters of parameters play a role. These are,

$$(d^2/\kappa d/\ell)^{\frac{1}{2}} / \hat{c} \quad \gamma_p'/\gamma_w \tan \hat{\theta} \quad c \tan \hat{\theta}$$

The influence of the last parameter is but small, as can be seen from equation (10.16), because  $c$  is small. If this is omitted it is clear that the quantity  $H(\ell)/L / (\gamma_p'/\gamma_w \tan \hat{\theta})$  depends only on the parameter,

$$\bar{c}(\ell) = (d^2/\kappa d/\ell)^{\frac{1}{2}} / \hat{c} \quad (10.18)$$

Using the technique of curve fitting the following approximate representation can be obtained,

$$H(\frac{1}{2}L)/L = \bar{c}(\frac{1}{2}L) \gamma_p'/\gamma_w \tan \hat{\theta} 0.98 [1 - 0.65 \bar{c}(\frac{1}{2}L)^{0.42}] \quad (10.19)$$

For practical engineering it is a truly simple tool. The accuracy is excellent within the range  $\bar{c} < 0.44$ . A similar less accurate formula can be determined for the value of  $H(L)$ ,

$$H(L)/L = \bar{c}(L) \gamma_p'/\gamma_w \tan \hat{\theta} 0.60 \quad \bar{c} < 0.22 \quad (10.20)$$

Due to  $\bar{c}$  it is obvious that the critical hydraulic head  $H(\frac{1}{2}L)$  is fairly proportional to  $L^{\frac{1}{2}}$  rather than to be linear as is often assumed in the literature. If the stress state of the sand is not considered, proportion to  $L^{\frac{1}{2}}$  should be obtained, Sellmeijer (1981).

## 11. Practical Aspects

### 11.1. Introduction

The problem of piping so far has been studied in this thesis from a theoretical viewpoint only. It has been found that the mechanism can be described by combining classical theories such as groundwater flow, limit equilibrium, hydraulics and particle mechanics. In addition, a design formula has been derived which resembles the rules of Bligh (1910) or Lane (1935), but which is based on theoretical assumptions rather than empiricism. This formula relates soil properties to hydraulic head and seepage length and is presented in (10.19). Such a theoretical study however has value if and only if it serves practical interests. This chapter deals with practical aspects in general and the application of formula (10.19) in particular.

The practice of dike supervision has put forward a number of questions: Which particular events due to piping have taken place during the past and under which circumstances? If the threat of piping is realistic at a certain location, what measures can be taken to reduce the probability of calamities? In case there is a certain governmental policy enforced for dike supervision one will emphasize to draft guidelines. These will also have to include what to do if a current location does not exactly match the assumptions in theory and/or codes.

These questions will be encountered in the next three sections. The first one will deal with classification, the second with mitigative measures. The last section presents recommendations for guidelines.

### 11.2. Classification

In order to chart the piping problem an inventory of the relevant aspects has to be drawn up. These are: typical failures, scope of

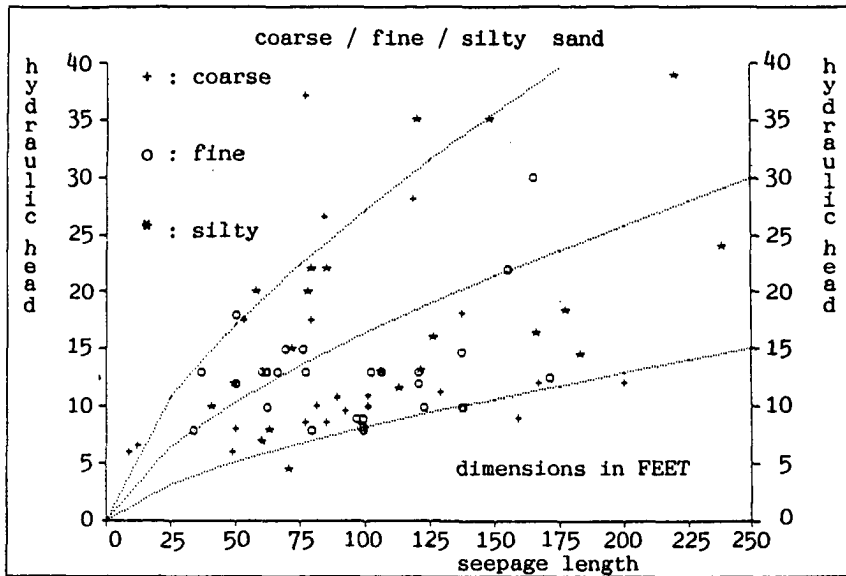


Fig. 11.1 : General dam failures [Lane]

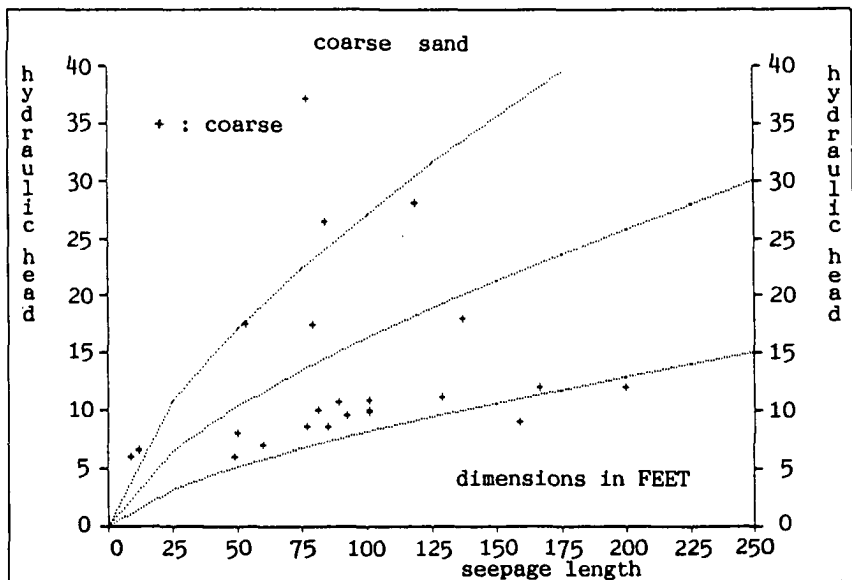


Fig 11.2 : Dam failures in coarse sand [Lane]



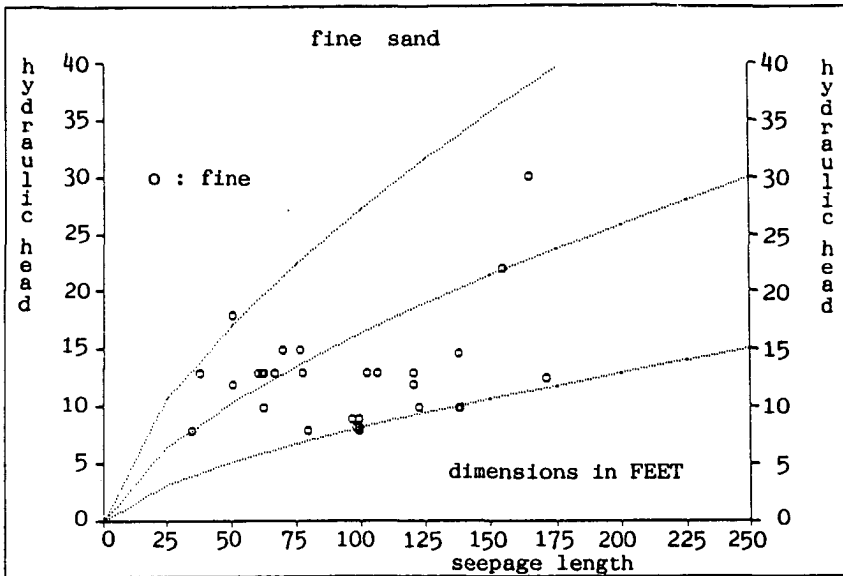


Fig. 11.3 : Dam failures in fine sand [Lane]

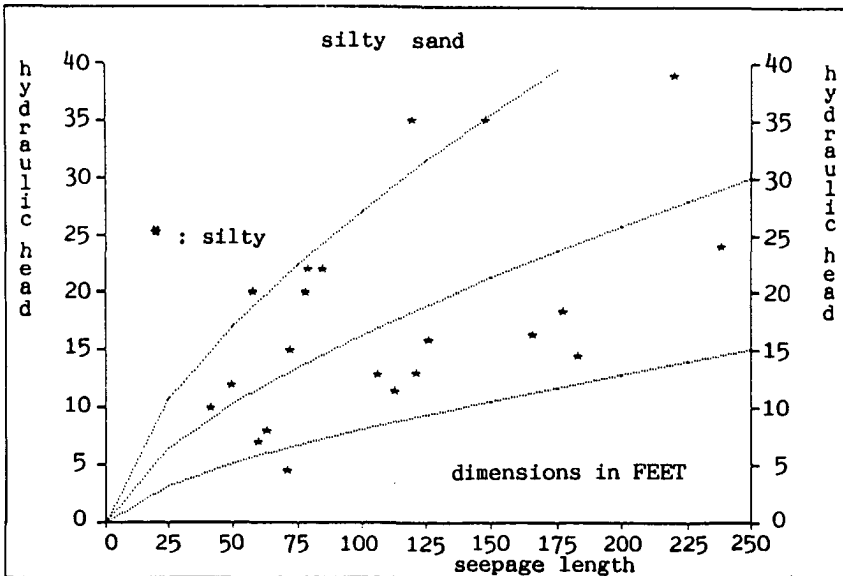


Fig 11.4 : Dam failures in silty sand [Lane]

methods, safety and relevant site investigation. They will be considered separately.

#### 11.2.1 Failures

To begin with, historical disasters due to piping are mentioned. The majority of these piping calamities refers to dams. A great number is reported by Lane (1935). As these are quite instructive they are presented in figures 11.1 ... 11.4, in which for each failure case the hydraulic head and the seepage length are plotted. The first graph shows all calamities grouped together regardless of reported soil conditions or geometry. In the remaining three pictures the cases of coarse (+), fine (o) and silty (\*) subsoil conditions are separately shown. The dotted lines are given for reference. They are two third power functions of head and length and correspond to a normal variation in sandy soils. In chapter 10 it was found that this relation describes the influence of the geometry, according to the theory presented in this thesis.

The scatter is mainly due to a very wide range of soil conditions. It is apparent that the shape of the dotted lines encloses quite well the reported failures. This fact supports the design rule (10.19). It is a matter of regret that the soil descriptions are insufficient. But still, interesting conclusions can be drawn.

A possible drawback of the design formula (10.19) is that it is sensitive to soil parameters such as permeability, which are often uncertain or hard to determine. One is apt to take recourse to the rules of Bligh or Lane (2.01), where a fixed coefficient is employed, based on a visual impression of soil alone. In table I, which is presented in the next paragraph, these coefficients are summarized. Apparently it is suggested that a certain type of soil, e.g. medium sand, has a fixed influence on piping, independent of its typical soil characteristics. It is clear from the figures 11.1 ... 11.4 that this would be wrong. The itemized graphs for a certain soil type show a scatter in the same order as

the combined graph without distinction with respect to soil type. In reality soil properties vary considerably and so should the coefficients of Bligh and Lane.

And there is more to be noticed. The coarse sand picture 11.2 contains a few questionable readings. Actually, these would fit in the silty sand graph much better. Many of the soil details suggested in figures 11.02 ... 11.04, however, most likely will have been specified without laboratory or site testing, but based on the experience of the site engineer alone. It is clear that with respect to piping this may lead to a subjective classification and consequently to a wrong coefficient.

It is obvious that a great deal of attention must be paid to a proper determination of soil characteristics. Formula (10.19) specifies which soil parameters play a major role and which impact they have on the coefficient. Imperical estimates of the coefficient, as suggested in table I, are deceptive and should be applied with great care. As a matter of fact, the engineer should find an optimum between designing conservatively and a more balanced approach based on site investigation rather than to hide uncertainty behind a fixed coefficient.

Another category of piping events concerns river and sea dikes, especially in delta areas. Here, occurrence of a disaster is less sudden, because of the appearance of the so-called sandboils, located often close to the inner toe of the dike. They consist of sand transferred from below the body of the dike. In the middle of these boils the sand is fluidized due to outflowing water. Under the dike body a slit has formed while sand is eroded away to form sandboils. This slit is, most likely, similar to what Lane (1935) calls the 'line of creep'.

The sandboil/slit system within certain boundaries plays the role of a regulating valve. If the hydraulic head across the dike increases, the slit becomes slightly longer and deeper and the sandboil higher, always trying to reach the state of equilibrium. However, the system has its limits, when these are reached it may

# EMPIRICAL

$$L/H = E \quad (11.1)$$

---

$$E \text{ [Bligh]} : (L = L_{\text{horizontal}})$$

Riverbeds of light silty sand	18
Fine micaceous sand	15
Coarse-grained sand	12
Boulders or shingle and gravel and sand	5 to 9

---

$$E \text{ [Lane]} : (L = L_{\text{vertical}} + \frac{1}{2} L_{\text{horizontal}})$$

Very fine sand or silt	8.5
Fine sand	7.0
Medium sand	6.0
Coarse sand	5.0
Fine gravel	4.0
Medium gravel	3.5
Coarse gravel, including cobbles	3.0
Boulders with some cobbles and gravel	2.5

---

# THEORETICAL

$$H/L = \frac{\gamma_p}{\gamma_w} \tan \hat{\theta} \bar{c} [1 - 0.65 (\bar{c})^{0.42}] \quad (11.2)$$

$$\bar{c} = (d^2 / \kappa \ 2d/L)^{\frac{1}{2}} / \hat{c}$$

---

## Soil Parameters :

$\frac{\gamma_p}{\gamma_w}$	: volumetric weight ratio
$\hat{\theta}$	: bedding angle
$\hat{c}$	: drag factor
$\kappa/d^2$	: normalized intrinsic permeability
$d$	: particle diameter ( $d_{15}$ to $d_{75}$ )

Tab. I : Available design rules

result in collapse of the complete structure. It is good practice to monitor the behaviour of sandboils regularly and to be alert for adverse changes in the phenomenon. Counter measures can then be taken in due time, since there is little time to spare when the equilibrium is disturbed.

A good example of a delta area with dikes sensitive to piping is The Netherlands. Numerous sandboils are found along the river and estuary dikes. Small, big and huge sandboils are a sometimes threatening picture. But in history, a few disasters only are believed to have been caused by piping. The reason that these dikes are relatively safe against piping is the fact that their base is rather long so as to meet other design criteria such as stability and that the sandboil/slit valve-system appears to be effective.

#### 11.2.2 Design methods

The majority of the dikes and dams has been designed applying the rules of Bligh and Lane (2.01). These rules contain empirical coefficients which are summarized in table I. As mentioned in the previous paragraph these coefficients do not reflect the relevant soil characteristics but they are based on the soil type only. They are therefore deceptive and should be used with great care.

Since there is a tendency for optimum design, engineers go on searching for methods that depend on objective parameters, which can be determined from site and laboratory testing. A first trial was performed by Müller-Kirchenbauer (1978), de Wit et al. (1981) and Hannes et al. (1985). Steady state groundwater flow solutions were calibrated against results of laboratory scale model tests.

The method has been applied e.g. in connection with the project of the Oosterschelde storm surge barrier. Under extreme storm conditions this barrier will close off the river estuary from the sea exposing the inner dike-system around the basin to a stagnant waterlevel. During a period of several days this situation must be

safe against piping. It turned out that the method resulted in very conservative predictions due to the fact that it does not contain the safety valve mechanism of the sandboil/slit combination.

Next, the theoretical study of the mechanism of piping, presented in this thesis, was undertaken. This resulted in a design formula of the form of equation (10.19). This formula is numerically of a very simple nature and more or less resembles the rules of Bligh and Lane. The big difference, however, is the fact that the coefficient  $E$  in (2.01) is now specified in terms of soil parameters rather than an empirical soil classification. In table I the rule (2.01) of Bligh and Lane is copied as (11.1) and the theoretical formula (10.19) is presented as (11.2).

It has already been mentioned when discussing figures 11.1 ... 11.4 that it is not a straightforward procedure to estimate the coefficient  $E$ . Also, quite often the soil parameters in (11.2) have to be determined by engineering judgement. But after having

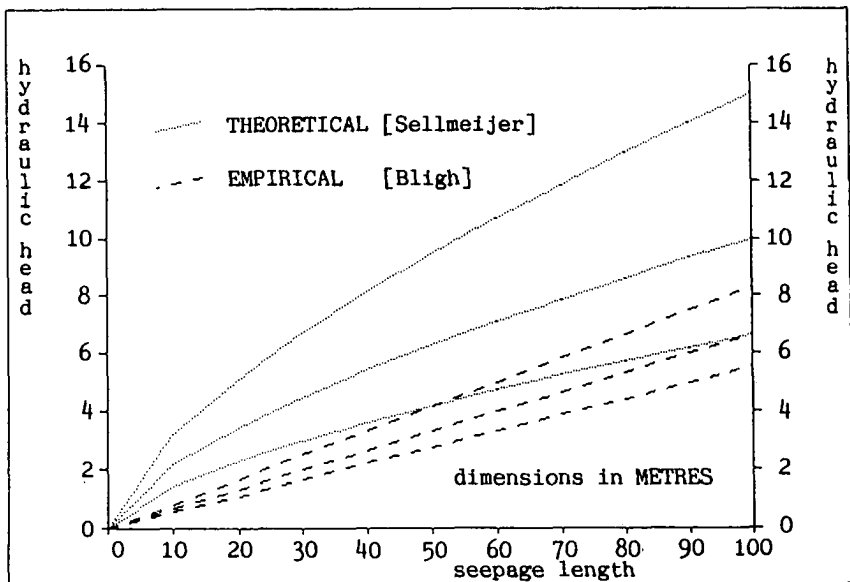


Fig 11.5 : Comparison between empirical and theoretical results

refined the soil estimates, one will notice that formula (11.2) consistently allows for a higher hydraulic head across the structure than the one following from the empirical rules. The basic assumption so far has been that formula (11.2) predicts values at which collapse becomes a fact, that is it includes no safety margin. This is not clear for the rules of Bligh and Lane, although there are indications that the authors meant it to be that way. In figure 11.5 a fair comparison between the theoretical and empirical approach is presented. In the results obtained with (11.2) the influence of permeability is considered too, what leads to a wider range than the results obtained with (11.1) show.

### 11.2.3. Safety

An important feature of piping prediction is safety. Which safety is required and how is it defined? Two definitions are common. A deterministic one, which is simply a factor which is applied to the calculated ultimate strengths to obtain a certain safety margin. The other one is a (semi) probabilistic approach, which takes into account the probability of collapse. In the latter analysis a certain probability of failure, which depends on aspects of personal and economic nature, is acceptable.

The deterministic method is the conventional one. In the Dutch polders the rules of Bligh and Lane have been applied successfully without considering additional safety coefficients. This means that these rules actually predict safe circumstances. It can be concluded from figure 11.5 that the introduction of a safety factor of 1.5 to 2.5 in formula (11.2) would be appropriate, if formula (11.2) is tuned to coincide with the rules of Bligh and Lane.

A deterministic safety factor actually is a strange quantity. A factor of 1.5 for instance seems sufficient, but does not provide any information about the sensitivity of the weakest link. A much better method is the probabilistic approach. Here the variation of each parameter of the piping formula is traced and

taken into account. Employing statistical methods an overall failure probability can be determined, which has to be balanced against the allowable risk prescribed by law or regulation. Such an approach is being undertaken for formula (11.2), the results will be reported in the near future.

#### 11.2.4. Site investigation

In order to apply formula (11.2) fundamental knowledge of the soil parameters and soil condition is necessary. The essential parameters are,

- volumetric weight ratio,  $\gamma_p/\gamma_w$
- bedding angle,  $\hat{\theta}$
- drag factor,  $\hat{C}$
- normalized intrinsic permeability,  $\kappa/d^2$
- particle diameter,  $d$  ( $d_{60}$  to  $d_{10}$ )

To measure the volumetric weight in the laboratory is daily routine. There are several techniques of more or less undisturbed sampling in situ. Determined values are quite reliable and hardly any variation has to be taken into account. The same is true for the particle diameter. A grain size distribution is obtained from sieve analysis. The three other parameters, however, require more effort.

The bedding angle and drag factor should be measured in a laboratory test set-up. White (1940), Martin (1970) and Fernandez Luque and Van Beek (1976) have performed tests from which these quantities can be derived. These tests are no daily routine; they are expensive and time-consuming. Too few experimental data are available at this moment. Values of the bedding angle ranging from  $49^\circ$  to  $63^\circ$  are measured and the drag factor may be interpreted to amount 3 to 4. No estimation of the variability is made. In order to design against piping a wider range of experimental data is necessary.



More is known, however, about the intrinsic permeability. Several empirically or theoretically based representations are presented in literature. A simple and for the design of piping quite appropriate one is  $\kappa/d_{10}^2 = \beta$ , Bear (1978). The value of  $\beta$  is 0.0045 for clayey sand and 0.014 for pure sand, while 0.010 is suggested as an average. Since the relation appears as a one third power in the piping criterion the variability plays a moderate role in a probabilistic approach.

If there is need for a more precise estimation of the permeability in-situ tests must be performed. These have to be carried out in such a way that the total discharge of the groundwater flow is involved, which can be achieved by monitoring at several locations the head in the sandy layer during changes in the outer water level. In river areas this can be done during an upcoming flood; in tidal areas during a 13 hour period of tidal movement. The value of the permeability can be obtained by applying an appropriate flow theory (Barends 1987).

In general the dike management is not familiar with detailed soil investigation and therefore often reluctant to carry it out. Without proper soil data, however, the uncertainty in the soil parameters is quite large and this consequently leads to very massive dikes or expensive mitigative measures to cope with the problem of piping. The aim should be to seek the optimum of the total cost of engineering and soil investigation on the one hand, and of construction management and mitigative action on the other hand, given an acceptable probability of failure. A minimum of soil data is always required, otherwise it is not possible to estimate the uncertainty in the soil parameters.

### 11.3. Mitigative measures

Now that the piping phenomenon has been classified into relevant aspects such as failure, methods, safety and soil testing, the next question is what can be done to avoid its threat. In a

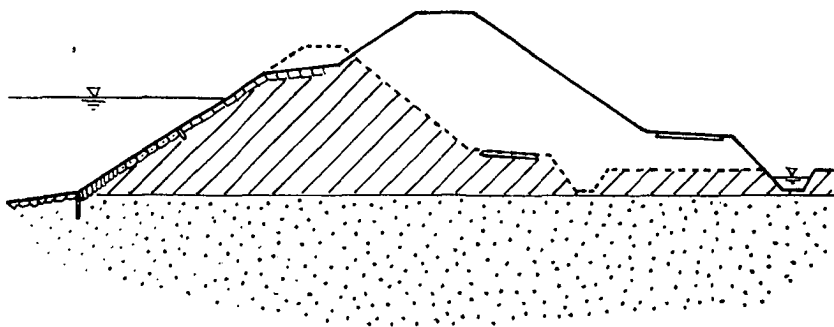


Fig. 11.6 : Typical dike improvement

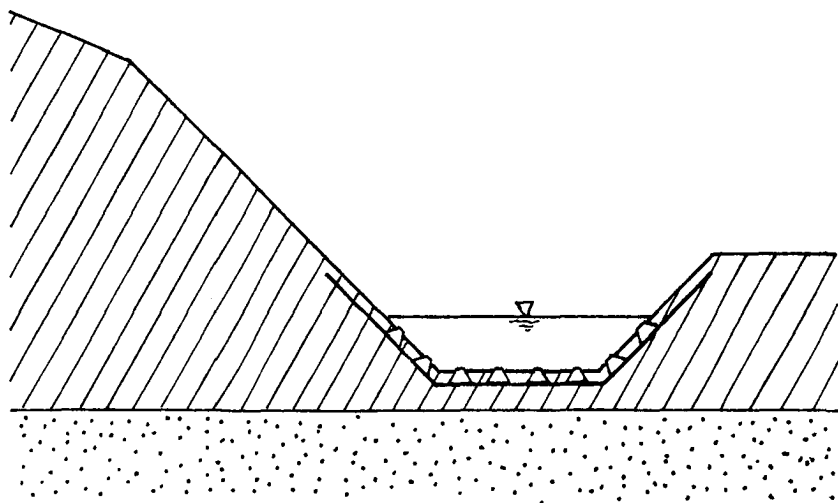


Fig 11.7 : Putting in textiles

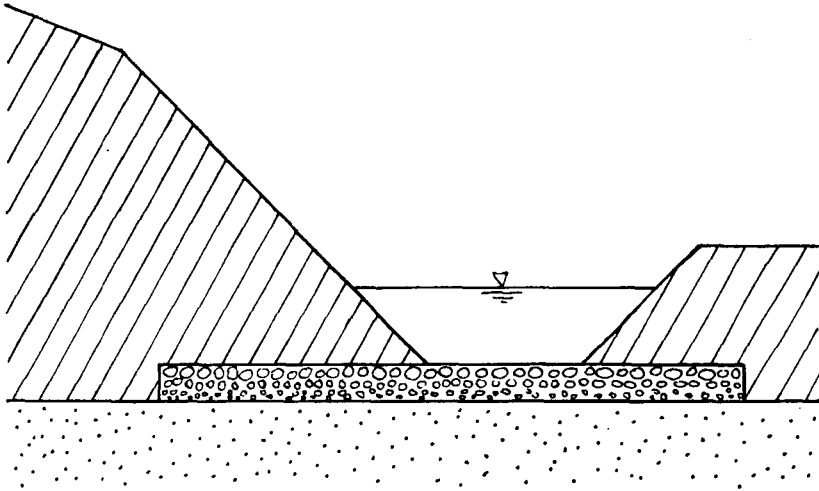


Fig. 11.8 : Use of filters

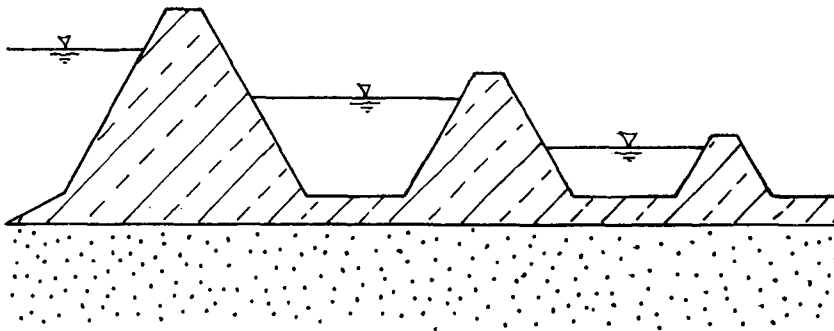


Fig 11.9 : Application of seepage dams

mechanical system of equilibrium there are always two components. On the one hand there is the active force (load) - which in case of piping is the hydraulic head across the structure - and on the other hand the strength of the structure determined by the geometry and the soil parameters. The hydraulic head is usually a given factor. It is a statistical quantity and not really open to design. But the reaction strength can be modified. There are several effective measures which may be taken to tackle the piping threat. The most important ones are:

- 1) extension of the seepage length
- 2) application of textiles
- 3) utilization of filters
- 4) use of seepage dams
- 5) sheet pile walls

ad 1) The conventional method in case of dikes is to simply make the dike wider. This is effective as can be observed from formula (11.2) or from the linear rules of Bligh or Lane. The approach is mostly part of a major program of dike improvement. To meet stricter requirements regarding safety against overflow the dikes are raised. For stability reasons they should then get a wider base, which at the same time provides more resistance to piping. There are several other reasons why dikes often have a wide base. In addition to stability the phenomenon of overflow due to waves requires moderate slopes and often an inspection road at the inner toe of the dike is constructed. An impression of a typical dike improvement is presented in figure 11.6 .

Compared to other materials soil is not particularly expensive, but large quantities have to be moved around and the result can be a very massive structure. It is not always desirable to extend dikes. Through the years houses have been built along the existing dikes and personal estates lie

adjacent to it. Interference with the historical situation is a time-consuming and painful matter.

ad 2) Textiles are a rather new material in soil mechanics. They can perform a number of functions such as separation, filtering and reinforcement. If the location from where piping is initialized is known, e.g. in a ditch, then textiles are a possible means to prevent piping due to the filtration property. The application is relatively simple, also in the case of existing dike structures. In figure 11.7 an example is shown. It is a cheap, effective and elegant solution, but it is vulnerable to mechanical damage. Since ditches must be cleaned up regularly, it is not unlikely that the textile is ruptured or torn during the cleaning process by mechanical means, thereby losing its intended function. Therefore, only textiles which have been protected with concrete strips or blocks should be applied. Maintenance must be regularly carried out.

ad 3) An alternative is the use of a filter. This is a layer of granular material with increasing particle size towards the surface. Figure 11.8 shows the outline. Good filters are difficult to make. The problem is the process of suffusion. This is the transport of smaller particles through a matrix of larger ones. The intention of a filter is to increase the resistance to erosion at the surface by diminishing the seepage pressures acting against the bigger more resistant particles. Suffusion might hamper this process.

Filters are much more expensive than textiles. However, they have an important advantage. If filters are properly designed, they fulfil the valve function just like the sandboil/slit system does. Textiles do not have this property. Since the pressure remains intact, the problem might shift to a weak location of the surface behind the dike. As for the problem of cleaning up ditches, filters are

less sensitive to damage than textiles. They are still effective even if minor changes to the surface are made. But just as for textiles maintenance of filters should be performed periodically.

ad 4) The application of seepage dams is an interesting but somewhat odd solution. It is only relevant in vast areas without a specific designation. Figure 11.9 shows the principle. Behind the main dike a series of dikes with decreasing height is constructed. The soil material is semi-permeable and more or less erosion proof. In case of flooding, the spaces in between the dikes will inundate, supplying enough counter pressure to avoid the piping process. In Hungary, along some parts of river Danube (Donau), this method has been applied successfully. In densely populated delta areas this method is not appropriate, because a lot of valuable land is lost.

ad 5) The last method, the use of sheet piles is used very frequently in the case of dams. Lane (1935) developed his formula for this particular case, distinguishing between horizontal and vertical permeability. Terzaghi (1967) reported on studies employing flow net theory. Harza (1935) introduced the electric analogy method in dam design. If sheet piles are applied at the inner toe of a dam than piping is no longer a problem, but heave might threaten the structure's stability.

For dikes and embankments, however, a solution by sheet piles is hardly ever applied. In the past other methods have been preferred, yet it is a suitable way of controlling piping, for example in the case of natural or artificial reservoirs just behind the dike. Such a situation might exist at a location of a previous dike collapse. Just behind the dike a relatively deep pond is left over after dike

restoration. None of the remaining mitigative measures are effective here.

#### 11.4 Suggestions for guidelines

A challenging step forward in piping analysis is to draw up guidelines for the design and monitoring procedures. This should not be considered to be a simple matter. On the one hand an instruction set as detailed as possible must be drafted up, but on the other hand there must be room for creative design. There are a number of aspects which are important to define the guidelines. These are,

- qualified design rules and formulae
- risk analysis
- extent of site and laboratory investigation
- preferred mitigative measures
- monitoring systems

The number of design tools is very limited. There are only two kinds: The empirical rules of Bligh and Lane (11.1) and the theoretically based formula presented in this thesis (11.2). Both these tools are numerically of a very simple nature.

It is expected that in the long run formula (11.2) will yield more precise predictions than the empirical ones. This is due to the fact that specific soil parameters are more comprehensible than, without disrespect, sniffing at soil. At this stage, however, it is not wise to abolish the conventional rules completely, since a lot of experience has been acquired in the past. During the teething troubles of putting the rather new theoretical formula to practice, this will be of great use.

A problem arises if the soil stratification and the geometry of the dike is essentially more complex than those for which the

mentioned formula is derived. Often an impervious sublayer exists. What is its impact on the predictions? This item can be included by modifying the followed calculus in this thesis. The analysis is being carried out by Delft Geotechnics. The result will be published in the near future.

Other new developments have to be undertaken in close cooperation with the site engineers. They have to report specific wishes and inadequacies. If it is believed that a large impact is to be expected on the design formulae, their suggestions can be incorporated into the calculus of this thesis. However, a much more complex piping rule probably is then encountered - a rule of the shape of equations (9.01) ... (9.08) rather than of formula (11.2). A presentation of the results in table form may then be adequate.

The next two items, safety and soil investigation, depend very much on the economic standards and state of technology. They are related to each other with respect to cost. The price of soil testing and site investigation often is amply counterbalanced by the excess construction cost. As for the safety it is advisable to work with the probabilistic method rather than with the deterministic one. The application of the theory is not complicated and a sophisticated picture of all the influences of the different soil parameters is easily obtained. The allowed probability of failure must be defined for a certain location by law or regulation. This figure has a great impact on the scope of the work and the extent of the soil investigation.

A topic of interest is the kind of mitigative measures which is to be preferred. It is difficult to qualify a particular one as the best. But from a practical point of view the following notes can be made. A very reliable measure is to enlarge the width of the dike. It is technically sound and extra maintenance is not necessary. Often extension is already included in programs of dike improvement.



As a specific solution in certain locations one of the other types of measures can be applied. Textiles are cheap, effective, not labour intensive and not hostile to the environment. Often the use of a granular filter is preferred because there is a wide experience with their application. Sheet piles or slurry walls are scarcely applied to dikes; yet their use may be appropriate.

A last remark must be made about monitoring dikes and embankments. Regulations about this specific task are most important. There are three reasons why this has to be done. First it is necessary that the design formula is tested in situ. Second, information must be obtained for future improvements. Third, in case of dike failure due to piping, information must be available to reconstruct the process leading to collapse. In the past this task has been given too little attention.

## 12. Conclusions

From the fact that there is quite a good correspondence between the theoretical predictions and the experimental findings it may be concluded that the method of describing the piping phenomenon as put forward in this thesis has potential. Both the mechanism and the order of magnitude appear to be well reproduced. Simple design diagrams that follow from the approximations of the more complicated general theory will allow the design engineer to propose structures and to investigate the sensitivity of variations in the expected soil parameters and dimensions of the structure.

Apparently certain weaknesses in the analysis, such as two-dimensionality and the neglect of higher order terms, do not seriously affect the validity of the outcome. In spite of the fact that the investigation was carried out on geometrics appropriate to the available laboratory tests, there is no reason not to modify the calculus to include other, in practice more frequently occurring, set-ups. Especially the influence of an impervious layer of subsoil at some depth below the structure has practical relevance and needs further investigation. Another rather more complicated situation is the one where the structure is punctured at some distance downstream. The latter situation contains a three-dimensional aspect, but the main elements discussed in this thesis - limiting soil stability combined with groundwater flow analysis and the possibility of localised particle transport - would certainly be applicable. As such this thesis may serve as a worthwhile case study, the salient points of which break new ground.

Acknowledgement

The author is indebted to Dr. M. A. Koenders for his editing advice. The enthusiasm of Mrs. R. H. Maguire in helping to put the typescript into plain English is gratefully acknowledged.

The technical and financial support of the Roads and Hydraulic Division of Rijkswaterstaat has been of great help.

## References

- (1902) Experiments on the Passage of Water through Sand  
Clibborn, J. and Beresford, J.S. , Govt. of India,  
Central Printing Office.
- (1910) Dams Barrages and Weirs on Porous Foundations  
Bligh, W.G. , Engineering News, p. 708 .
- (1913) The Stability of Weir Foundations on Sand and Soil Subject  
to Hydrostatic Pressure  
Griffith, W.M. , Minutes of Proceedings J.C.E. , Vol. 197  
pt III, p. 221 .
- (1935) Uplift and Seepage under Dams on Sand  
Harza, L.F. , Proceedings ASCE , Paper no. 1920 .
- (1935) Security from Under-Seepage Masonry Dams on Earth  
Foundations  
Lane, E.W. , Transactions ASCE , Vol. 100 ,  
Paper no. 1919 .
- (1940) The Equilibrium of Grains on the Bed of a Stream  
White, C.W. , Proceedings Royal Society London,  
Vol. 174A .
- (1945) Hydrodynamics  
Lamb, H. , Cambridge at the University Press,  
Dover Publ. , Inc. .
- (1960) Complex Variables and Applications  
Churchill, R.V. , McGraw-Hill Book Company, Inc. .

- (1961) Etude Mécanique d'un Milieu Pulvérulent Formé de Sphères égales de Compacité Maxima  
Dantu, P. , Actes du Cinquième Congrès International de Mécanique des Sols et des Travaux de Fondations, Paris.
- (1962) Piping Resistant Non Cohesive Soils  
Lubochkov, E.A. , Isvestia VN II G 71(1962), pp 61-89 .
- (1962) Theory of Groundwater Movement  
Polubarinova-Kochina, P.Ya. , Princeton University Press, Princeton, New Jersey.
- (1962) The Stress Dilatancy Relation  
Rowe, P. , proceedings Royal Society, London Series, vol. 269, pp 500-527 .
- (1967) Partial Differential Equations  
Garabedian, P.R. , John Wiley & Sons, Inc. , New York.
- (1967) Soil Mechanics in Engineering Practice  
Terzaghi, K. and Peck, R.B. , Wiley International Edition, John Wiley & Sons, Inc., New York, London, Sydney.
- (1968) Handbook of Mathematical Functions  
Abramowitz, M. and Stegun, I.A. , Dover Publications, Inc. , New York.
- (1970) Analyse III  
Duparc, H.J.A. and Herwaarden, F.G. , Handleiding College A50 , Delft University of Technology.
- (1970) Effect of a Porous Sand Bed on Incipient Motion  
Martin, C.S. , Water Resources Research, Vol. 6 no. 4 , pp. 1162-1174 .

- (1970) Theory of Groundwater Flow  
Verruijt, A. , MacMillan and Co Ltd, London.
- (1975) Integraltafel Teil I und II  
Gröbner, W. and Hofreiter, N. , Springer-Verlag, Wien,  
New York.
- (1976) Erosion and Transport of Bed-Load Sediment  
Fernandez Luque, R. and Van Beek, R. ,  
Journal of Hydraulic Research, 14 no. 2 , pp 127-144 .
- (1978) Hydraulics of Groundwater  
Bear, J. , McGraw-Hill, ISBN 0-07-004170-9 .
- (1978) Rückschreitende Erosion unter Bindiger Deckschicht  
Miesel, D. , Vorträge der Baugrundtagung, Berlin,  
Deutsche Gesellschaft für Erd- und Grundbau E. V. .
- (1978) Zum Zeitlichen Verlauf der Rückschreitenden Erosion in  
Geschichtetem Untergrund unter Dämmen und Stauanlagen  
Müller-Kirchenbauer, H. , Beitrag zum Talsperrensymposium,  
München.
- (1979) Vloeistofmechanica  
De Vries, M. , Handleiding College B72 ,  
Delft University of Technology.
- (1979) Design and Construction on Territories Subjected to Karst-  
Piping Processes in Moscow  
Dykhovichnyi, Yu.A. and Maksimenko, V.A. ,  
Soil Mechanics and Foundation Engineering  
(Osnovaniya)16(1979)3 , pp. 147-151 .
- (1981) Laboratory Study of Hydraulic Fracturing  
Seed, H.B. , Journal of Geotechnical Engineering Division,  
Proceedings ASCE , Vol. 107 , no. GT6 , June, 1981 .

- (1981) Piping due to Flow towards Ditches and Holes  
Sellmeijer, J.B. , Proceedings of Euromech 143 , Delft,  
pp. 69-72 .
- (1981) Seepage Erosion Analysis of Structures  
Van Zyl, D. and Harr, M.E., Proceedings of the Tenth  
International Conference on Soil Mechanics and Foundation  
Engineering, Stockholm, Part 1 , p. 503 .
- (1981) Laboratory Testing on Piping  
De Wit, J.M. , Sellmeijer, J.B. and Penning, A. ,  
Proceedings of the 10th International Conference on Soil  
Mechanics and Foundation Engineering, Stockholm, Part 1 ,  
p. 517 .
- (1983) An Introduction to Fluid Mechanics  
Batchelor, G.K. , Cambridge University Press, Cambridge
- (1985) Zur Mechanik der Rückschreitenden Erosion unter Deichen und  
Dämmen  
Hannes, U., Müller-Kirchenbauer, H. and Stavros, S.,  
Bautechnik 5 , pp. 163-168 .
- (1986) Special Shape Functions in Boundary Integral Method  
Sellmeijer, J.B. , Proceedings of the 8th International  
Conference on Boundary Element Methods in Engineering,  
Tokyo.
- (1987) A New Approach to Evaluate Pumping Test Data  
Barends, F.B.J. , Calle, E.O.F. , Weijers, J.B.A. ,  
9th conference ECSMFE , Dublin.
- (1987) Hydraulic Criteria for Protective Filters  
Koenders, M. A. , private communication.

A. Derivation of hypergeometric shape functions

In this appendix a possible relation for the true behaviour in the transition zones of the piping problem will be determined. There are three such zones; around  $x = 0$ ,  $x = b$  and  $x = l$ . It will appear that the character in all zones is equal. Therefore, one function only must be determined, for example the one around  $x = 0$ . From equation (9.01) it follows that this function must satisfy the condition that the nature of a variation of both  $p$  and  $q$  around  $x = 0$  is the same, provided  $x$  is positive.

A straightforward derivation of the desired relation is rather complicated, but it is quite likely that its behaviour will be a power function. In order to see if such a relation meets the condition of equal variation the following will be put forward,

$$p_{\epsilon} = \bar{p} \left(\frac{x}{l}\right)^{\epsilon} = \bar{p} x^{\epsilon} \quad 0 < x < 1 \quad (\text{A.01})$$

The strength of this contribution is denoted by  $\bar{p}$ . The dimensionless parameter  $x$  is introduced for reasons of convenience. The corresponding behaviour of  $q$  follows by substitution of the assumed value of  $p_{\epsilon}$  into equation (9.03). Two ways can be followed here. One may expand  $p_{\epsilon}$  into a Fourier series and determine  $q_{\epsilon}$  from the obtained coefficients. If  $p_{\epsilon}$  is extended to a power series this method yields good results. But one may also substitute  $p_{\epsilon}$  directly into the integral representation, which is preferred here for reasons of efficiency and elegance. Then a dimensionless expression is obtained by assuming  $\rho = r/l$ , remembering that  $x = x/l$ ,

$$q_{\epsilon} = \frac{\bar{p}}{\pi} \int_0^1 \rho^{\epsilon} \sqrt{\frac{1-x}{1-\rho}} \frac{d\rho}{\rho-x} \quad (\text{A.02})$$

This result is valid for  $x < 1$ . For the moment, only values of  $0 < x < 1$  are considered. The relation (A.02) appears to be a



hypergeometric function. The theory of these functions, denoted by  $F$ , is sufficiently summarized in Abramowitch and Stegun (1968), chapter 15. From now on all formulas starting with 15.3. refer to Abramowitch and Stegun (1968), chapter 15. Expressing  $q_\epsilon$  in such a function is very suitable in order to isolate the behaviour around  $x = 0$ . According to formula 15.3.1  $q_\epsilon$  may be written:

$$q_\epsilon = -\frac{\beta}{\pi} \frac{\sqrt{(1-x)}}{x} \frac{\Gamma(\frac{1}{2}) \Gamma(1+\epsilon)}{\Gamma(\frac{1}{2}+\epsilon)} F[1, 1+\epsilon; \frac{1}{2}+\epsilon; 1/x] - i \beta x^\epsilon \quad (A.03)$$

$$0 < x < 1$$

It must be noted that formula 15.3.1 contains a residue that has to be subtracted, since equation (A.02) is Cauchy integrated. The present shape of the relation (A.03) is not very suitable for numerical interpretation. Therefore, at first the complex term will be eliminated and the result rewritten. Using formula 15.3.9  $q$  may be expressed as,

$$q_\epsilon = -\frac{\beta}{\pi} \sqrt{(1-x)} \frac{\Gamma(-\frac{1}{2}) \Gamma(1+\epsilon)}{\Gamma(\frac{1}{2}+\epsilon)} F[1, \frac{1}{2}-\epsilon; \frac{1}{2}; 1-x] \quad (A.04)$$

$$0 < x < 1$$

For, it holds that  $F[\frac{1}{2}+\epsilon, 0; \frac{1}{2}; 1-x] = 1$ . Moreover, the value of the gamma function  $\Gamma(\frac{1}{2})$  is equal to  $\sqrt{(\pi)}$ . The real valued result (A.04) can be worked out by use of formula 15.3.6,

$$q_\epsilon = \frac{\beta}{\pi} \sqrt{(1-x)} \frac{\Gamma(\frac{1}{2}) \Gamma(\epsilon)}{\Gamma(\frac{1}{2}+\epsilon)} F[1, \frac{1}{2}-\epsilon; 1-\epsilon; x] - \beta x^\epsilon \cot(\pi\epsilon) \quad (A.05)$$

$$0 < x < 1$$

To obtain this equation use is made of the reflection formula for gamma functions,  $\Gamma(\epsilon) \Gamma(1-\epsilon) = \pi \csc(\pi\epsilon)$ . Moreover, according to formula 15.1.8 it holds that  $F[\frac{1}{2}, 1+\epsilon; 1+\epsilon; x]$  is equal to  $1 / \sqrt{(1-x)}$ . Finally the result may be polished by use of formula 15.3.3,

$$q_{\epsilon} = \frac{\beta}{\pi} \frac{\Gamma(\frac{1}{2}) \Gamma(\epsilon)}{\Gamma(\frac{1}{2}+\epsilon)} F[-\epsilon, \frac{1}{2}; 1-\epsilon; x] - \beta x^{\epsilon} \cot(\pi\epsilon) \quad (A.06)$$

$$0 < x < 1$$

Indeed this is the hoped-for result. The hypergeometric function in (A.06) is very smooth around  $x = 0$ , so, if  $0 < \epsilon < 1$ , the second expression in equation (A.06) defines the variation in  $q_{\epsilon}$  for small values of  $x$ . And this expression has the same character as equation (A.01). In appendix B it will be shown how the value of  $\epsilon$  can be determined from the conditions of limit equilibrium.

A satisfactory result has been obtained. It must be noted that the behaviour of  $q_{\epsilon}$  is of the order of  $\sqrt{(1-x)}$ . But this does not affect the results. After all the calculation can be performed on the  $\xi$ -scale, defined by (9.05). After having defined the type of function of  $p_{\epsilon}$  all other important features can be determined. The integral representation of the vertical gradient (9.03) is also valid for  $x < 0$  without need of Cauchy's principle. That means that formula (A.02) may be applied again. However, the hypergeometric notation does not contain a residue for  $x < 0$ . Formula (A.03) now has the form,

$$q_{\epsilon} = -\frac{\beta}{\pi} \frac{\sqrt{(1-x)} \Gamma(\frac{1}{2}) \Gamma(1+\epsilon)}{x \Gamma(\frac{1}{2}+\epsilon)} F[1, 1+\epsilon; \frac{3}{2}+\epsilon; 1/x] \quad x < 0 \quad (A.07)$$

This is a real valued function. For better understanding of its behaviour the expression is rewritten by use of formula 15.3.7. The following is then obtained:

$$q_{\epsilon} = \frac{\beta}{\pi} \sqrt{(1-x)} \frac{\Gamma(\frac{1}{2}) \Gamma(\epsilon)}{\Gamma(\frac{1}{2}+\epsilon)} F[1, \frac{1}{2}-\epsilon; 1-\epsilon; x] - \beta (-x)^{\epsilon} \csc(\pi\epsilon) \quad (A.08)$$

$$x < 0$$

Again the reflection formula for gamma functions and formula 15.1.8 are applied. The equation (A.08) is a very beautiful result. Together with the relation (A.06) it clearly shows the behaviour of  $q_{\epsilon}$  around  $x = 0$ . Unfortunately the hypergeometric

function in (A.08) is not fully appropriate for numerical interpretation, since the absolute value of the argument  $x$  can exceed unity. But in that case equation (A.07) can be applied successfully. The results (A.07) and (A.08) are rewritten using formula 15.3.3 and the following is obtained:

$$q_{\epsilon} = \frac{\beta}{\pi} \frac{\Gamma(\frac{1}{2}) \Gamma(\epsilon)}{\Gamma(\frac{1}{2} + \epsilon)} F[-\epsilon, \frac{1}{2}; 1 - \epsilon; x] - \beta (-x)^{\epsilon} \csc(\pi\epsilon) \quad (A.09)$$

$-1 < x < 0$

$$q_{\epsilon} = \frac{\beta}{\pi} \sqrt{-\frac{1}{x}} \frac{\Gamma(\frac{1}{2}) \Gamma(1 + \epsilon)}{\Gamma(\frac{1}{2} + \epsilon)} F[\frac{1}{2} + \epsilon, \frac{1}{2}; \frac{1}{2} + \epsilon; 1/x] \quad x < -1 \quad (A.10)$$

The vertical gradient is sufficiently defined by equations (A.06), (A.09) and (A.10). The next important feature to be determined is the discharge per unit permeability, expressed in equation (9.04). It contains the value of the head. Since the horizontal gradient is defined by assumption (A.01), the head simply follows by integration. Then the value of  $Q$  in dimensionless variables is defined by,

$$Q_{\epsilon} = -\frac{\beta \ell}{\pi} \int_0^1 \frac{\rho^{1+\epsilon}}{1+\epsilon} \sqrt{\frac{1-x}{1-\rho}} \frac{d\rho}{\rho-x} + \frac{2\beta \ell}{\pi} \sqrt{1-x} \int_0^1 \rho^{\epsilon} \frac{d\rho}{\sqrt{1-\rho}} \quad (A.11)$$

If one reduces the  $1+\epsilon$  power of  $\rho$  in the first integral by replacing  $\rho$  by  $\rho-x+x$ , the result contains the expression for the vertical gradient defined in (A.02). This simplifies the expression of  $Q$  to,

$$Q_{\epsilon} = -\frac{x}{1+\epsilon} q_{\epsilon} + \frac{2\beta \ell}{\pi} \frac{1+\epsilon}{1+\epsilon} \sqrt{1-x} \int_0^1 \rho^{\epsilon} \frac{d\rho}{\sqrt{1-\rho}} \quad (A.12)$$

Integration of the remaining integral is not difficult. It is a degeneration of a hypergeometric function. By use of formula

15.3.1 the expression of  $Q_\epsilon$  can be further worked out, bearing in mind that  $F[0, 1+\epsilon; \frac{1}{2}+\epsilon; x] = 1$ ,

$$Q_\epsilon = -\frac{x}{1+\epsilon} q_\epsilon + \frac{2\beta\ell}{\pi} \frac{\int(1-x)}{1+\epsilon} \frac{\Gamma(\frac{1}{2}) \Gamma(1+\epsilon)}{\Gamma(\frac{1}{2}+\epsilon)} \quad (A.13)$$

It turns out that once the value of the vertical gradient is determined, the value of the discharge can be obtained quite simply.

The remaining quantity to be specified is the hydraulic head across the structure, defined by equation (9.07). As in the case of  $Q_\epsilon$  this feature can be worked out as follows,

$$H_\epsilon = -\frac{\beta\ell}{\pi} \int_0^1 \frac{\rho^{1+\epsilon}}{1+\epsilon} \sqrt{\frac{\lambda-1}{1-\rho}} \frac{d\rho}{\rho-\lambda} + \frac{2\beta\ell}{\pi} \sqrt{\lambda-1} \int_0^1 \rho^\epsilon \frac{d\rho}{\sqrt{(1-\rho)}} \quad (A.14)$$

where  $\lambda$  denotes  $L/\ell$ . Again the  $1+\epsilon$  power in the first integral is reduced. Remembering the result of the second integral, which is the same as in (A.12) the equation (A.14) may be rewritten,

$$H_\epsilon = -\frac{\beta\ell}{\pi} \int_0^1 \frac{\rho^\epsilon}{1+\epsilon} \sqrt{\frac{\lambda-1}{1-\rho}} \frac{d\rho}{\rho-\lambda} + \frac{2\beta\ell}{\pi} \frac{\sqrt{\lambda-1}}{1+\epsilon} \frac{\Gamma(\frac{1}{2}) \Gamma(1+\epsilon)}{\Gamma(\frac{1}{2}+\epsilon)} \quad (A.15)$$

The remaining integral is nothing less than the value of the horizontal gradient in  $x = L$ . For, it follows from equation (5.04) that if  $z = L$  with  $L > \ell$ ,

$$p(L) = -\frac{1}{\pi} \int_0^\ell p(r) \sqrt{\frac{L-r}{\ell-r}} \frac{dr}{r-L} \quad (A.16)$$

Choosing for  $p(r)$  the power function defined in (A.01) and normalizing all quantities of dimension length on to  $\ell$  yields,

$$p_{\epsilon}(L) = - \frac{\tilde{p}}{\pi} \int_0^1 \rho^{\epsilon} \sqrt{\frac{\lambda-1}{1-\rho}} \frac{d\rho}{\rho-\lambda} \quad (\text{A.17})$$

Again a hypergeometric function is recognized. The same procedure as for  $q_{\epsilon}$  can be followed in the case of  $x < 0$ . Analogous to the derivation from (A.02) via (A.07) to (A.10) the following expression is obtained:

$$p_{\epsilon}(L) = \frac{\tilde{p}}{\pi} \int \left(\frac{1}{\lambda}\right) \frac{\Gamma(\frac{1}{2}) \Gamma(1+\epsilon)}{\Gamma(\frac{1}{2}+\epsilon)} F[\frac{1}{2}+\epsilon, \frac{1}{2}; \frac{1}{2}+\epsilon; \frac{1}{\lambda}] \quad (\text{A.18})$$

This quantity can be used to determine the value of  $H_{\epsilon}$ , since it follows from (A.15) ... (A.17) that,

$$H_{\epsilon} = \frac{L}{1+\epsilon} p_{\epsilon}(L) + \frac{2\tilde{p}l}{\pi} \frac{\sqrt{\lambda-1}}{1+\epsilon} \frac{\Gamma(\frac{1}{2}) \Gamma(1+\epsilon)}{\Gamma(\frac{1}{2}+\epsilon)} \quad (\text{A.19})$$

By now all important features describing the groundwater flow are expressed in the form of the true behaviour of the solution around  $x = 0$ . In the next appendix these contributions will be worked out for the three different transition zones.

B. Application of hypergeometric shape functions

In the previous appendix the character of the true behaviour of the solution around the transition zones has been determined. It turned out that this behaviour is well described by a set of hypergeometric shape functions. In this appendix it will be shown that these functions can be used in all transition zones. Each zone has its own shape parameter  $\epsilon$ .

There are three transition zones: around  $x = 0$ ,  $x = b$  and  $x = l$ . The problem is to determine the value of  $\epsilon$  from the relation between the variations in  $p$  and  $q$ . The zones  $x = 0$  and  $x = l$  are quite simple to handle; the zone  $x = b$  will turn out to be complicated and troublesome.

At first the zone  $x = 0$  is considered. There, for  $x > 0$ , equation (9.01) is valid. In  $x = 0$  the value of  $p$  is 0 and that of  $q$  is  $\gamma_s'/\gamma_w$ . If small variations in  $p$  and  $q$  are denoted by  $\delta p$  and  $\delta q$ , so that  $p = \delta p$  and  $q = \gamma_s'/\gamma_w - \delta q$ , then equation (9.01) yields the following relation:

$$\delta q \approx \delta p \cot \theta \quad (\text{B.01})$$

If a variation of  $p$  of the type (A.01) is supposed then the corresponding variation of  $q$  follows from (A.06). The first term, the hypergeometric function, is rather smooth. So the variation is determined by the second term. Therefore the following relation is valid,

$$\delta q \approx \delta p \cot(\pi \epsilon) \quad (\text{B.02})$$

When comparing equations (B.01) and (B.02) the assumed variations prove to be well chosen, because these equations are identical if  $\epsilon = \theta/\pi$ . The value of  $\epsilon$  in  $x = 0$  will be denoted by  $\epsilon_0$ , with,

$$\epsilon_0 = \theta/\pi \quad (\text{B.03})$$

Thus the hypergeometric shape functions of appendix A describe for this value of  $\epsilon$  the behaviour of the solution around  $x = 0$ .

The next zone to be investigated is that around  $x = \ell$ . At first it must be made clear that the solution has a symmetrical form. Up till now  $p(x)$  is the unknown function and all other features are expressed in this item. But one may also assume  $q(\ell-x)$  to be the unknown function. A similar system of relations is obtained, except that now for  $p$  and  $P$  read  $q$  and  $Q$ , and vice versa.

To prove this mathematically for the integral expression some calculation is needed. But if one rewrites the Fourier expressions of (9.03) and (9.04) as function of  $1-\xi$  and considers the transformation equation (9.05) for  $\ell-x$  and  $1-\xi$ , then the reflection procedure becomes clear.

Having realized this, the variations in the transition zone  $x = \ell$  can be considered. Here, for  $x < \ell$ , equation (9.02) is valid. In  $x = \ell$  the value of  $q$  is 0 and that of  $p$  is  $\gamma_p/\gamma_w \cot\theta$ . Moreover  $Q$  vanishes. If small variations in  $p$ ,  $q$  and  $Q$  are denoted by  $\delta p$ ,  $\delta q$  and  $\delta Q$  respectively, so that  $p = \gamma_p/\gamma_w \cot\theta - \delta p$ ,  $q = \delta q$  and  $Q = \delta Q$ , then equation (9.02) yields the following relation:

$$C \delta q + \frac{1}{2} C [12 \kappa/d^2 (\gamma_p/\gamma_w)^2 \cot^2 \theta \delta Q/d]^{\frac{1}{2}} \approx \delta p \cot \hat{\theta} \quad (\text{B.04})$$

For reflected shape functions the variation of  $q$  is supposed to be of the type (A.01), but with  $\bar{p}$  replaced by  $\bar{q}$  and  $x$  by  $1-x$ . Then the variation  $\delta Q$  simply follows from integration. The result is proportional to  $(1-x)^{1+\epsilon}$ . Thus the first term of (B.04) is of the form  $(1-x)^\epsilon$  and the second one of the form  $(1-x)^{\frac{1}{2}(1+\epsilon)}$ . Since  $\frac{1}{2}(1+\epsilon) > \epsilon$ , provided that  $\epsilon < \frac{1}{2}$  (which must be checked later), the second term of the equation (B.04) can be neglected compared to the first one. That means that equation (B.04) may be simplified to,

$$C \delta q \approx \delta p \cot \hat{\theta} \quad (\text{B.05})$$

As the variations  $\delta q$  and  $\delta p$  follow from equation (A.01) and the second term of equation (A.06), again with  $\tilde{p}$  replaced by  $\tilde{q}$  and  $x$  by  $1-x$ , it may be written,

$$\delta p \approx \delta q \cot(\pi\epsilon) \quad (\text{B.06})$$

The equations (B.05) and (B.06) are identical if  $\cot(\pi\epsilon)$  is equal to  $C \tan\theta$ . If the value of  $\epsilon$  in  $x = \ell$  is denoted by  $\epsilon_\ell$ , the final result is,

$$\epsilon_\ell = \frac{1}{2} - \arctan(C \tan\theta) / \pi \quad (\text{B.07})$$

Indeed it holds that  $\epsilon_\ell < \frac{1}{2}$ . The reflected hypergeometric shape functions of appendix A for this value of  $\epsilon$  describe the behaviour of the solution around  $x = \ell$ .

Up till now the procedure has been quite straightforward. However, the derivation of shape functions for the third transition zone - around  $x = b$  - will be less tractable. The procedure will be the same as above: first assume a possible behaviour of shape functions, then define the condition for the variations and subsequently examine if the prescribed condition is satisfied. A possible behaviour of shape functions will be assumed by combining the following functions of the normal and reflected type,

$$p_\epsilon = \tilde{p}_b \left( \frac{x-b}{\ell-b} \right)^{\epsilon_b} \quad b < x < \ell$$

and, (B.08)

$$q_\epsilon = -\tilde{q}_b \left( \frac{b-x}{b} \right)^{\epsilon_b} \quad 0 < x < b$$

Here, the subscript  $b$  denotes the zone around  $x = b$ . The first equation yields hypergeometric shape functions as described in appendix A; the second one produces reflected ones.



After having assumed the equations (B.08) the behaviour of the variations around  $x = b$  can be written down. As before, a variation in  $p$  is denoted by  $\delta p$  and one in  $q$  by  $\delta q$ . Using (A.01), (A.06) and (A.08) it follows,

$$\delta p = \bar{q}_b \left( \frac{b-x}{b} \right)^{\epsilon_b} \cot(\pi \epsilon_b) \quad \lim x \rightarrow b \quad (B.09)$$

$$\delta q = -\bar{q}_b \left( \frac{b-x}{b} \right)^{\epsilon_b} - \bar{p}_b \left( \frac{b-x}{\ell-b} \right)^{\epsilon_b} \csc(\pi \epsilon_b)$$

$$\delta p = \bar{p}_b \left( \frac{x-b}{\ell-b} \right)^{\epsilon_b} + \bar{q}_b \left( \frac{x-b}{b} \right)^{\epsilon_b} \csc(\pi \epsilon_b) \quad \lim x \rightarrow b \quad (B.10)$$

$$\delta q = -\bar{p}_b \left( \frac{x-b}{\ell-b} \right)^{\epsilon_b} \cot(\pi \epsilon_b)$$

The behaviour around  $x = b$  is uniquely defined by equations (B.09) and (B.10). The next step of the procedure will now be carried out: impose conditions for the variations. These conditions are nothing more than the equations (9.01) and (9.02). The first one is valid for  $x < b$ ; the second for  $x > b$ . They are now expressed in terms of variations and therefore a differentiation in the point  $b$  is carried out. It is convenient to multiply (9.01) by  $q$  first. The variation of  $Q$  in (9.02) is of a higher order and may be neglected. The result is as follows:

$$(2 \gamma_w / \gamma_s \bar{q}_b - 1) \delta q + \delta p \cot \theta = 0 \quad x < b \quad (B.11)$$

$$C \delta q + \delta p \left( \frac{1}{2} \hat{C} \bar{a}_b / d + 1 \right) \cot \hat{\theta} = 0 \quad b < x \quad (B.12)$$

The fact that the results depend on the actual values of  $q$  and  $a$  in point  $b$  is a complicating factor. At the outset these are unknown values.

The last stage of the procedure consists of an examination as to whether conditions (B.11) and (B.12) can be met. To that end the variations (B.09) and (B.10) will be substituted in these conditions. In so doing the following conditions are obtained,

$$\bar{q}_b \left\{ \frac{\cot\theta}{2 \gamma_w / \gamma_s q_b - 1} \cot(\pi \epsilon_b) - 1 \right\} = \bar{p}_b \left( \frac{b}{\ell - b} \right)^{\epsilon_b} \csc(\pi \epsilon_b) \quad (B.13)$$

$$\bar{p}_b \left\{ \frac{C \tan\hat{\theta}}{\frac{1}{2} \hat{C} a_b / d + 1} \cot(\pi \epsilon_b) - 1 \right\} = \bar{q}_b \left( \frac{\ell - b}{b} \right)^{\epsilon_b} \csc(\pi \epsilon_b) \quad (B.14)$$

It is noted that multiplying (B.13) and (B.14) leads to a condition for  $\cot(\pi \epsilon_b)$  only. That means that a value of  $\epsilon_b$  can be obtained independent of the weights of the shape functions. The fact that this value depends on  $q_b$  and  $a_b$  is rather inconvenient but not a problem. After having specified the value of  $\epsilon_b$  one condition is left which relates the weights of the applied shape functions. Apparently there is only one degree of freedom in point  $b$  just like in the other two transition points.

In order to make the structure more transparent auxiliary parameters  $\bar{\mu}$  and  $\mu$  are defined as follows,

$$\tan \bar{\mu} = (2 \gamma_w / \gamma_s q_b - 1) \tan \theta \quad -\theta < \bar{\mu} < \theta \quad (B.15)$$

$$\tan \mu = (\frac{1}{2} \hat{C} a_b / d + 1) / C \tan \hat{\theta} \quad \frac{1}{2} \pi - \pi \epsilon_\ell < \mu < \frac{1}{2} \pi$$

When assessing the range of values of  $\bar{\mu}$  and  $\mu$  it is kept in mind that  $0 < q_b < \gamma_s / \gamma_w$  and that  $a_b > 0$ . Remember that  $\epsilon_\ell$  is determined by (B.07). Applying (B.15) to (B.13) and (B.14) the following set of equations is obtained:

$$[\cot \bar{\mu} \cot(\pi \epsilon_b) - 1] \bar{q}_b (\ell-b)^{\epsilon_b} = \bar{p}_b (b)^{\epsilon_b} \csc(\pi \epsilon_b) \quad (B.16)$$

$$[\cot \mu \cot(\pi \epsilon_b) - 1] \bar{p}_b (b)^{\epsilon_b} = \bar{q}_b (\ell-b)^{\epsilon_b} \csc(\pi \epsilon_b)$$

Multiplying the first of (B.16) by the second of (B.16) results in an equation in  $\cot(\pi \epsilon_b)$  only. Note that  $\csc^2(\pi \epsilon_b)$  is equal to  $1 + \cot^2(\pi \epsilon_b)$ , so,

$$[\cot \bar{\mu} \cot(\pi \epsilon_b) - 1] [\cot \mu \cot(\pi \epsilon_b) - 1] = 1 + \cot^2(\pi \epsilon_b) \quad (B.17)$$

This is a square equation and there are two solutions. One is  $\epsilon_b = \frac{1}{2}$ , representing the trivial solution corresponding to no variations. The other one is determined:

$$\cot(\pi \epsilon_b) = \frac{\cot \bar{\mu} + \cot \mu}{\cot \bar{\mu} \cot \mu - 1} = \tan(\bar{\mu} + \mu) = \cot(\frac{1}{2}\pi - \bar{\mu} - \mu) \quad (B.18)$$

No continuous result is guaranteed by (B.18). The difficulty arises for values of  $\epsilon_b$  close to unity when the cotangent jumps. Clearly in this area the shape functions cannot be used because the variations as expressed by the power functions attain a linear character. The approximation made is then no longer valid in that the smooth part of the shape functions interferes and becomes of the same order as the variational part. It can be demonstrated that in this region of material parameters the whole shape function becomes logarithmic in character.

Not all the information encased in equations (B.16) has been used. A relationship between the weights  $\bar{p}_b$  and  $\bar{q}_b$  can be ascertained. Multiplication of both members of the first equation of (B.16) by  $\sin \bar{\mu} \sin(\pi \epsilon_b)$  yields,

$$[\cos \bar{\mu} \cos(\pi \epsilon_b) - \sin \bar{\mu} \sin(\pi \epsilon_b)] \bar{q}_b (\ell-b)^{\epsilon_b} = \bar{p}_b (b)^{\epsilon_b} \sin \bar{\mu}$$

or equivalently,

$$\cos(\bar{\mu} + \pi \epsilon_b) \bar{q}_b (\ell - b)^{\epsilon_b} = \bar{p}_b (b)^{\epsilon_b} \sin \bar{\mu} \quad (\text{B.19})$$

If the second equation of (B.16) was considered rather than the first one then a synonymous relation would have been obtained,

$$\cos(\mu + \pi \epsilon_b) \bar{p}_b (b)^{\epsilon_b} = \bar{q}_b (\ell - b)^{\epsilon_b} \sin \mu \quad (\text{B.20})$$

The conditions laid down in (B.16) are met if the equations (B.18) and (B.19) or (B.20) are satisfied which is possible, since from these equations an independent value of  $\epsilon_b$  can be determined. One degree of freedom for the weight is ensured.

Summarizing, it can be stated that hypergeometric shape functions may be applied to assist in the construction of the complete solution in all three transition zones. In the zones around  $x = 0$  and  $x = \ell$  the powers as they occur in equations (B.03) and (B.07) are known from the outset because they depend on soil parameters only. In the zone around  $x = b$  the power depends on the value of the vertical gradient and the depth of the slit as well. Moreover its behaviour is not always continuous and its application appears to be unreliable for values close to unity. In the latter case the shape function need not be added to the calculation process.

C. Elaboration of design formula

In this appendix some intermediate calculations will be carried out to determine a clear, though approximate, description of the piping mechanism. At first the assumed behaviour of the horizontal normalized gradient  $p$  (10.06) will be integrated with respect to  $x$ . Thus, because  $p = dP/dx$ , the normalized head  $P$  is obtained. Since  $x = x/\ell$  the following must be worked out,

$$\frac{P}{\ell} = \int_0^x \frac{dp}{(1-\rho)^\beta + c} \quad (C.01)$$

Using simple algebra by which terms are split up (C.01) may be arranged as, provided that  $\beta < \frac{1}{2}$ ,

$$\frac{P}{\ell} = \int_0^x \frac{dp}{(1-\rho)^\beta} - c \int_0^x \frac{dp}{(1-\rho)^{2\beta}} + c^2 \int_0^x \frac{1}{(1-\rho)^\beta + c} \frac{dp}{(1-\rho)^{2\beta}} \quad (C.02)$$

The first two integrals are easily integrated. As the value of  $c$  is small the third integral may be neglected if  $x < 1$ . So the head behaves like,

$$\frac{P}{\ell} = \frac{1 - (1-x)^{1-\beta}}{1-\beta} - c \frac{1 - (1-x)^{1-2\beta}}{1-2\beta} \quad 0 \leq x < 1 \quad \beta < \frac{1}{2} \quad (C.03)$$

But if  $x = \ell$  or  $x = 1$  the third integral term in (C.02) is still significant. Therefore  $P(\ell)$  is defined by,

$$\frac{P(\ell)}{\ell} = \frac{1}{1-\beta} - \frac{c}{1-2\beta} + \int_0^1 \frac{c^2}{(1-\rho)^\beta + c} \frac{d\rho}{(1-\rho)^{2\beta}} \quad \beta < \frac{1}{2} \quad (C.04)$$

The problem is to calculate the integral term of this equation. This will be done as follows: indicate the integral by  $I$ , split

off integration from  $-\infty$  to 0 and substitute in the remaining integral  $1-\rho = c^{1/\beta} \exp(2\mu)$ . Then the third term of (C.04) may be written as,

$$I = c^{\frac{1}{\beta}-1} \int_{-\infty}^{\infty} \frac{2 \exp\{(2-5\beta)\mu\}}{\exp(\beta\mu) + \exp(-\beta\mu)} d\mu - \int_{-\infty}^0 \frac{c^2}{(1-\rho)^\beta + c} \frac{d\rho}{(1-\rho)^{2\beta}} \quad (C.05)$$

This representation is valid only if  $\frac{1}{2} < \beta < \frac{3}{2}$ . After slight rearrangement the first integral is a standard one; the second may be expanded into a geometric series,

$$I = c^{\frac{1}{\beta}-1} \int_{-\infty}^{\infty} \frac{\exp\{(2-5\beta)\mu\} + \exp\{-(2-5\beta)\mu\}}{\exp(\beta\mu) + \exp(-\beta\mu)} d\mu - \sum_{m=2}^{\infty} \int_{-\infty}^0 \frac{(-1)^m c^m d\rho}{(1-\rho)^{\beta(m+1)}} \quad \frac{1}{2} < \beta < \frac{3}{2} \quad (C.06)$$

The first integral is found in Gröbner and Hofreiter (1975) part II, 311, 11a. The second integral can be easily performed. Only the first term is relevant because  $c$  is small.

$$I = c^{\frac{1}{\beta}-1} \frac{\pi}{\beta} \csc\left\{\frac{\pi}{\beta}\right\} - \frac{c^2}{3\beta-1} \quad \frac{1}{2} < \beta < \frac{3}{2} \quad (C.07)$$

Eventually the final form of the head  $P(\ell)$  when substituting (C.07) into (C.04) becomes,

$$\frac{P(\ell)}{\ell} = \frac{1}{1-\beta} - \frac{c}{1-2\beta} - \frac{c^2}{3\beta-1} + c^{\frac{1}{\beta}-1} \frac{\pi}{\beta} \csc\left\{\frac{\pi}{\beta}\right\} \quad \frac{1}{2} < \beta < \frac{3}{2} \quad (C.08)$$

One wonders why so much effort is used to obtain this expression. This can be illustrated by rearranging (C.08) in two ways as follows:

$$\frac{\underline{P}(\ell)}{\ell} = \frac{1}{1-\beta} - \frac{c}{\beta} \frac{\beta}{1-2\beta} \left[ 1 - c^{\frac{1-2\beta}{\beta}} \pi \frac{1-2\beta}{\beta} \csc\left(\pi \frac{1-2\beta}{\beta}\right) \right] - \frac{c^2}{3\beta-1}$$

$$\frac{1}{2} < \beta < \frac{1}{2} \quad (C.09)$$

$$\frac{\underline{P}(\ell)}{\ell} = \frac{1}{1-\beta} - \frac{c^{\frac{1}{\beta}-1}}{\beta} \frac{\beta}{3\beta-1} \left[ c^{\frac{3\beta-1}{\beta}} - \pi \frac{3\beta-1}{\beta} \csc\left(\pi \frac{3\beta-1}{\beta}\right) \right] - \frac{c}{1-2\beta}$$

Some interesting limits become transparent now,

$$\lim_{\beta \rightarrow \frac{1}{2}} \frac{\underline{P}(\ell)}{\ell} = 2 (1 + c \ln c - c^2) \approx 2 (1 + c \ln c) \quad (C.10)$$

$$\lim_{\beta \rightarrow \frac{1}{2}} \frac{\underline{P}(\ell)}{\ell} = 3 \left( \frac{1}{2} - c - c^2 \ln c \right) \approx 3 \left( \frac{1}{2} - c \right)$$

It is clearly understood that, if  $\beta$  is significantly smaller than  $\frac{1}{2}$ , then for  $x \neq \ell$  the approximation (C.03) can be used successfully as well. But, if  $\beta$  approaches  $\frac{1}{2}$ , the result (C.08) must be used since it incorporates the logarithmic behaviour.

Next, integration of equation (10.08) is performed,

$$\frac{Q_0}{\ell} = \frac{2}{\pi} \int_0^1 \frac{1}{(1-\rho)^\beta + c} \sqrt{\frac{1}{1-\rho}} d\rho -$$

$$- \frac{1}{\pi} \int_0^1 \left[ \frac{1 - (1-\rho)^{1-\beta}}{1-\beta} - c \frac{1 - (1-\rho)^{1-2\beta}}{1-2\beta} \right] \frac{1}{\rho} \frac{d\rho}{\sqrt{(1-\rho)}} \quad \beta < \frac{1}{2} \quad (C.11)$$

The first integral, which will be written  $I_1$ , is similar to (C.01). Provided that  $\frac{1}{2} < \beta < \frac{1}{2}$ , it will be split up into three terms as follows:

$$\begin{aligned}
 I_1 = & \frac{2}{\pi} \int_0^1 \frac{d\rho}{(1-\rho)^{\beta+\frac{1}{2}}} - \frac{2}{\pi} \int_{-\infty}^1 \frac{c}{(1-\rho)^{\beta} + c} \frac{d\rho}{(1-\rho)^{\beta+\frac{1}{2}}} + \\
 & + \frac{2}{\pi} \int_{-\infty}^0 \frac{c}{(1-\rho)^{\beta} + c} \frac{d\rho}{(1-\rho)^{\beta+\frac{1}{2}}}
 \end{aligned} \quad (C.12)$$

Here, the first integration is easily carried out. In the second integral  $1-\rho = c^{1/\beta} \exp(2\mu)$  is substituted. The third one is expanded into a geometric series,

$$\begin{aligned}
 I_1 = & \frac{4}{\pi} \left[ \frac{1}{1-2\beta} - c^{\frac{1}{2\beta}-1} \int_{-\infty}^{\infty} \frac{\exp\{(1-3\beta)\mu\}}{\exp(\beta\mu) + \exp(-\beta\mu)} d\mu \right] + \\
 & + \frac{2}{\pi} \sum_{m=1}^{\infty} \int_{-\infty}^0 \frac{(-1)^{m+1} c^m d\rho}{(1-\rho)^{\beta(m+1)+\frac{1}{2}}}
 \end{aligned} \quad (C.13)$$

The first integral is a standard one and after a slight rearrangement found in Gröbner and Hofreiter (1975) part II, 311, 11a. From the second one only the first term is relevant, as  $c$  is small,

$$I_1 = \frac{4}{\pi} \left[ \frac{1}{1-2\beta} + c^{\frac{1}{2\beta}-1} \frac{\pi}{2\beta} \csc\left(\frac{\pi}{2\beta}\right) + \frac{c}{4\beta-1} \right] \quad (C.14)$$

In order to illustrate the behaviour of  $I_1$  for  $\beta$  close to  $\frac{1}{2}$  and  $\frac{1}{2}$  this result is rearranged as,

$$I_1 = \frac{4}{\pi} \left[ \frac{1}{2\beta} \frac{2\beta}{1-2\beta} \left\{ 1 - c^{\frac{1-2\beta}{2\beta}} \frac{1-2\beta}{2\beta} \csc\left(\pi \frac{1-2\beta}{2\beta}\right) \right\} + \frac{c}{4\beta-1} \right] \quad \frac{1}{2} < \beta < \frac{1}{2} \quad (C.15)$$

$$I_1 = \frac{4}{\pi} \left[ \frac{1}{1-2\beta} - c^{\frac{1}{2\beta}-1} \frac{2\beta}{2\beta} \frac{4\beta-1}{4\beta-1} \left\{ \pi \frac{4\beta-1}{2\beta} \csc\left(\pi \frac{4\beta-1}{2\beta}\right) - c^{\frac{4\beta-1}{2\beta}} \right\} \right]$$

The interesting limits are,



$$\lim_{\beta \rightarrow \frac{1}{2}} I_1 = \frac{4}{\pi} (-\ln c + c) \quad (C.16)$$

$$\lim_{\beta \rightarrow \frac{1}{2}} I_1 = \frac{8}{\pi} (1 + c \ln c)$$

For  $\beta \rightarrow \frac{1}{2}$  the behaviour becomes logarithmic as is to be expected.

So much for the first integral. The second one will be written  $I_2$  and according to (C.11) is characterized by,

$$I_2 = \frac{1}{\pi} \int_0^1 \left[ \frac{1 - (1-\rho)^{1-\beta}}{1-\beta} - c \frac{1 - (1-\rho)^{1-2\beta}}{1-2\beta} \right] \frac{d\rho}{\rho \sqrt{(1-\rho)}} \quad (C.17)$$

This relation will turn out to be a standard integral and is by substitution of  $1-\rho = \exp(-2\mu)$  transformed into,

$$I_2 = \frac{2}{\pi} \int_0^\infty \left[ \frac{1}{1-\beta} \frac{1 - \exp\{-2(1-\beta)\mu\}}{\exp(\mu) - \exp(-\mu)} - \frac{c}{1-2\beta} \frac{1 - \exp\{-2(1-2\beta)\mu\}}{\exp(\mu) - \exp(-\mu)} \right] d\mu \quad (C.18)$$

These integrals are to be found in Gröbner and Hofreiter (1975) part II, 311, 16,

$$I_2 = \frac{1}{\pi} \left[ \frac{\Psi(\frac{1}{2}-\beta) - \Psi(\frac{1}{2})}{1-\beta} - c \frac{\Psi(\frac{1}{2}-2\beta) - \Psi(\frac{1}{2})}{1-2\beta} \right] \quad (C.19)$$

Here,  $\Psi$  is the psi-function explained in e.g. Abramowitz and Stegun (1968).

The integrals  $I_1$  and  $I_2$  are now worked out. So an expression for the total discharge from the slit is found. Substitution of (C.14) and (C.19) into (C.11) finally yields,

$$\begin{aligned} \frac{Q_0}{\ell} = & \frac{4}{\pi} \left[ \frac{1}{1-2\beta} + c^{\frac{1}{2\beta}-1} \frac{\pi}{2\beta} \csc\left(\frac{\pi}{2\beta}\right) + \frac{c}{4\beta-1} \right] + \\ & - \frac{1}{\pi} \left[ \frac{\Psi\left(\frac{1}{2}-\beta\right) - \Psi\left(\frac{1}{2}\right)}{1-\beta} - c \frac{\Psi\left(\frac{1}{2}-2\beta\right) - \Psi\left(\frac{1}{2}\right)}{1-2\beta} \right] \end{aligned} \quad \frac{1}{2} < \beta < \frac{3}{2} \quad (C.20)$$

Lastly, integration of formula (10.11) is performed in order to obtain the critical head. It reads,

$$\begin{aligned} \frac{H(\frac{1}{2}L)}{L} = & \frac{1}{\pi} \int_0^1 \frac{1}{(1-\rho)^\beta + c} \sqrt{\frac{1}{1-\rho}} d\rho + \\ & + \frac{1}{2\pi} \int_0^1 \left\{ \frac{1 - (1-\rho)^{1-\beta}}{1-\beta} - c \frac{1 - (1-\rho)^{1-2\beta}}{1-2\beta} \right\} \frac{1}{2-\rho} \frac{d\rho}{\sqrt{(1-\rho)}} \end{aligned} \quad (C.21)$$

The first integral has already been solved and the result can be found in (C.14). In the second integral  $1-\rho = \exp(-2\mu)$  will be substituted,

$$\begin{aligned} \frac{H(\frac{1}{2}L)}{L} = & \frac{1}{2} I_1 + \\ & \frac{1}{\pi} \int_0^\infty \left[ \frac{1}{1-\beta} \frac{1 - \exp\{-2(1-\beta)\mu\}}{\exp(\mu) + \exp(-\mu)} - \frac{c}{1-2\beta} \frac{1 - \exp\{-2(1-2\beta)\mu\}}{\exp(\mu) + \exp(-\mu)} \right] d\mu \end{aligned} \quad (C.22)$$

The integral has a similar shape as (C.18). It will prove useful to combine them. Since  $I_1 - I_2 = Q_0/\ell$  (C.22) may be rearranged as,

$$\begin{aligned} \frac{H(\frac{1}{2}L)}{L} = & \frac{1}{2} \frac{Q_0}{\ell} + \\ & + \frac{1}{\pi} \int_0^\infty \left[ \frac{\exp(\mu)}{1-\beta} \frac{1 - \exp\{-2(1-\beta)\mu\}}{\exp(2\mu) - \exp(-2\mu)} - c \frac{\exp(\mu)}{1-2\beta} \frac{1 - \exp\{-2(1-2\beta)\mu\}}{\exp(2\mu) - \exp(-2\mu)} \right] d\mu \end{aligned} \quad (C.23)$$

Again this is a standard integral. With the aid of Gröbner and Hofreiter (1975) part II ,311 , 16 the equation becomes,

$$\frac{H(\frac{1}{2}L)}{L} = \frac{1}{2} \frac{Q_0}{L} + \frac{1}{2\pi} \left[ \frac{\Psi(\frac{1}{2}-\frac{1}{2}\beta) - \Psi(\frac{1}{2})}{1-\beta} - c \frac{\Psi(\frac{1}{2}-\beta) - \Psi(\frac{1}{2})}{1-2\beta} \right] \quad (C.24)$$

It is essential to consider the characteristic quantity  $Q_0/\frac{1}{2}L$  rather than  $Q_0/L$  , as  $\ell = \frac{1}{2}L$  . Due to the derivation of  $Q_0/\ell$  equation (C.24) is valid for  $\frac{1}{2} < \beta < \frac{1}{2}$  .

## Curriculum Vitae

30 april 1947	Geboren te Amsterdam
1959 - 1965	Gymnasium- $\beta$ aan het Ignatius-College te Amsterdam
1965	Aanvang studie aan de Afdeling der Civiele Techniek van de Technische Universiteit Delft
1968 - 1972	Assistent bij de Vakgroep Grondmechanica van de Technische Universiteit Delft
1969	Stage bij Karayollari Genel M $\ddot{u}$ d, Turkije; Laboratorium en veldwerk voor de wegenbouw en Turkse geschiedenis en cultuur
1972	Behalen van het Diploma van Civiel Ingenieur (cum laude) aan de Technische Universiteit Delft
1972 - 1973	Dienstverband bij het Centrum Onderzoek Water- keringen van Rijkswaterstaat; Onderzoek naar grondwaterstroming in dijken
1973 - 1975	Studie aan de Universiteit van Osaka betreffende de Japanse taal en cultuur; Studie aan de Universiteit van Kyoto betreffende grondwaterstroming
1975	Dienstverband bij Grondmechanica Delft
1975 - 1980	Project-Ingenieur bij de Speurwerk-afdeling
1980 - 1985	Groepshoofd Fundamenteel Onderzoek
1985 -	Wetenschappelijk Specialist